

Roadmap

Nanotechnology for catalysis and solar energy conversion

U Banin¹ , N Waiskopf¹, L Hammarström² , G Boschloo², M Freitag²,
E M J Johansson², J Sá² , H Tian² , M B Johnston³ , L M Herz³ ,
R L Milot⁴, M G Kanatzidis⁵ , W Ke⁵, I Spanopoulos⁵, K L Kohlstedt⁵ ,
G C Schatz⁵ , N Lewis⁶ , T Meyer⁷ , A J Nozik^{8,9} , M C Beard⁸ ,
F Armstrong¹⁰ , C F Megarity¹⁰, C A Schmuttenmaer^{11,12} ,
V S Batista^{11,13}  and G W Brudvig^{11,13} 

¹ The Institute of Chemistry and the Center for Nanoscience and Nanotechnology, The Hebrew University of Jerusalem, Jerusalem 91904, Israel

² Department of Chemistry—Ångström Laboratory, Uppsala University, Box 523, SE-75120 Uppsala, Sweden

³ Department of Physics, University of Oxford, Clarendon Laboratory, Parks Road, Oxford OX1 3PU, United Kingdom

⁴ Department of Physics, University of Warwick, Gibbet Hill Road, Coventry CV4 7AL, United Kingdom

⁵ Department of Chemistry, Northwestern University, Evanston, IL 60208, United States of America

⁶ Division of Chemistry and Chemical Engineering, and Beckman Institute, 210 Noyes Laboratory, 127-72 California Institute of Technology, Pasadena, CA 91125, United States of America

⁷ University of North Carolina at Chapel Hill, Department of Chemistry, United States of America

⁸ National Renewable Energy Laboratory, United States of America

⁹ University of Colorado, Boulder, CO, Department of Chemistry, 80309, United States of America

¹⁰ Department of Chemistry, University of Oxford, Oxford, United Kingdom

¹¹ Department of Chemistry, Yale University, 225 Prospect St, New Haven, CT, 06520-8107, United States of America

E-mail: uri.banin@mail.huji.ac.il, leif.hammarstrom@kemi.uu.se, michael.johnston@physics.ox.ac.uk, m-kanatzidis@northwestern.edu, kkohlstedt@northwestern.edu, g-schatz@northwestern.edu, nslewis@its.caltech.edu, tjmeyer@email.unc.edu, Arthur.Nozik@nrel.gov, fraser.armstrong@chem.ox.ac.uk, victor.batista@yale.edu and gary.brudvig@yale.edu

Received 11 May 2020, revised 11 September 2020

Accepted for publication 30 September 2020

Published 5 November 2020




CrossMark

Abstract

This roadmap on Nanotechnology for Catalysis and Solar Energy Conversion focuses on the application of nanotechnology in addressing the current challenges of energy conversion: ‘high efficiency, stability, safety, and the potential for low-cost/scalable manufacturing’ to quote from the contributed article by Nathan Lewis. This roadmap focuses on solar-to-fuel conversion, solar water splitting, solar photovoltaics and bio-catalysis. It includes dye-sensitized solar cells

¹² Guest editor of the Roadmap, deceased.

¹³ Guest editors of the Roadmap, to whom any correspondence should be addressed.

 Original content from this work may be used under the terms of the [Creative Commons Attribution 4.0 licence](https://creativecommons.org/licenses/by/4.0/). Any further distribution of this work must maintain attribution to the author(s) and the title of the work, journal citation and DOI.

(DSSCs), perovskite solar cells, and organic photovoltaics. Smart engineering of colloidal quantum materials and nanostructured electrodes will improve solar-to-fuel conversion efficiency, as described in the articles by Waiskopf and Banin and Meyer. Semiconductor nanoparticles will also improve solar energy conversion efficiency, as discussed by Boschloo *et al* in their article on DSSCs. Perovskite solar cells have advanced rapidly in recent years, including new ideas on 2D and 3D hybrid halide perovskites, as described by Spanopoulos *et al* ‘Next generation’ solar cells using multiple exciton generation (MEG) from hot carriers, described in the article by Nozik and Beard, could lead to remarkable improvement in photovoltaic efficiency by using quantization effects in semiconductor nanostructures (quantum dots, wires or wells). These challenges will not be met without simultaneous improvement in nanoscale characterization methods. Terahertz spectroscopy, discussed in the article by Milot *et al* is one example of a method that is overcoming the difficulties associated with nanoscale materials characterization by avoiding electrical contacts to nanoparticles, allowing characterization during device operation, and enabling characterization of a single nanoparticle. Besides experimental advances, computational science is also meeting the challenges of nanomaterials synthesis. The article by Kohlstedt and Schatz discusses the computational frameworks being used to predict structure–property relationships in materials and devices, including machine learning methods, with an emphasis on organic photovoltaics. The contribution by Megarity and Armstrong presents the ‘electrochemical leaf’ for improvements in electrochemistry and beyond. In addition, biohybrid approaches can take advantage of efficient and specific enzyme catalysts. These articles present the nanoscience and technology at the forefront of renewable energy development that will have significant benefits to society.

Keywords: renewables, biocatalysis, solar cells, solar energy conversion, water splitting, multiple exciton generation, photocatalysis

(Some figures may appear in colour only in the online journal)

Contents

1. Colloidal quantum materials as photocatalysts for solar to fuel conversion	3
2. Dye-sensitized solar cells	5
3. THz studies of nanomaterials for solar energy conversion	7
4. Perovskite solar cells	9
5. Multiscale computational methods for generating accurate nanoscale structures in OPV materials	11
6. Solar-driven water splitting	13
7. Surface-bound molecular assemblies on nanostructured electrodes for solar fuel generation	15
8. Multiple exciton generation (MEG) from hot carriers for solar energy conversion	18
9. Cascade biocatalysis in electrode nanopores	21

1. Colloidal quantum materials as photocatalysts for solar to fuel conversion

Nir Waiskopf and Uri Banin

The Institute of Chemistry and the Center for Nanoscience and Nanotechnology, The Hebrew University of Jerusalem, Jerusalem 91904, Israel

E-mail: uri.banin@mail.huji.ac.il

Status. Colloidal quantum materials composed of semiconductor-based nanoparticles have been suggested, more than a decade ago, as photocatalysts for the conversion of solar energy to chemical work. One of the main photocatalytic applications that have been investigated is water splitting, which aims to utilize the energy absorbed by the nanocrystals (NCs), to produce hydrogen gas along with oxygen, directly by reduction and oxidation of water, respectively. The hydrogen gas can then be reacted in a controlled manner with oxygen to form back water in a fuel cell providing electricity thus elegantly resulting in a zero-emission cycle.

The ability to tune and tailor the electronic band structure of the nanoparticles by size, shape, and composition, the large surface to volume ratio and the capacity to utilize the small particles directly in solution or embedded in a matrix have led to the exploration of various systems for water splitting, mostly, by separation of the two half-cell reactions. Moreover, the tunability of their properties allowed the execution of systematic studies to reveal the fundamental parameters which govern the performances and to decipher their mechanism of action.

The photocatalytic cycle comprises the following main steps: (1) The absorption of light; (2) the mobility of the charge carriers to the reaction site; (3) and the catalytic reaction. Each of them was found to depend on multiple parameters requiring fine-tuning to balance all the effects and optimize the efficiency of the system [1]. The main categorical parameters that were found to influence these steps are: (a) the composition and dimensions of the photocatalysts, that inherently determine their electronic and chemical properties, including the band offset and chemical stability, the over-potentials to the desired reactions as well as the reactivity and adsorption energy of the reagents to the catalytic site [2–4]; (b) the surface coating of the NCs which should provide sufficient dispersibility and passivate surface traps without interfering to the accessibility of the reagents to the reaction center [5–7]; (c) and the environmental conditions, that should be tuned to provide chemical and colloidal stability and on the other hand, were found to significantly affect the measured quantum yields [8, 9].

Current and future challenges. A homostructure NC has limited capacity to answer all the demands required for the challenging task of photocatalytic water splitting. However, significant efforts are invested to engineer an all-in-one system comprised of multiple components which by the right integration can manifest synergistic effects and fulfill all the

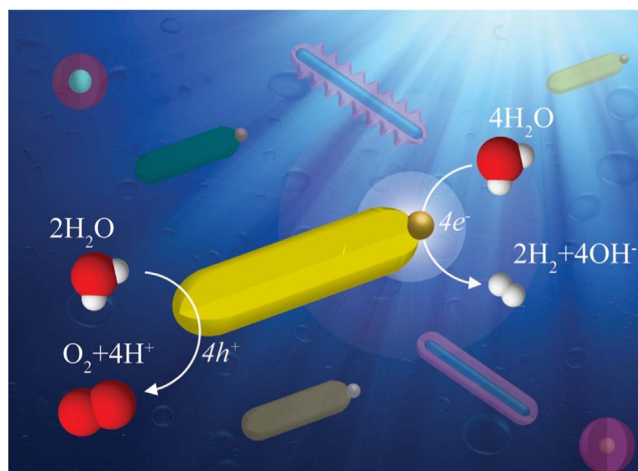


Figure 1. Artist's view of full water splitting by semiconductor-metal hybrid nanoparticle. The illustration presents the two half-reactions occurring on two distinct sites on a single particle. The background of the illustration emphasizes the capacity to utilize various nanocrystals that differ by size, shape, and composition.

requirements for an efficient solar to fuel conversion. Semiconductor heterostructures together with soluble co-catalysts and semiconductor-metal hybrid structures are two exemplary systems that were used to widen the photocatalyst's absorption range, prolong the lifetime of the excited charge carriers, increase their probability to reach the active sites and to optimize the catalytic process [10, 11]. Moreover, smart engineering of the nanoparticles surface coating, for example by linking molecular co-catalysts to the surface of the nanoparticles [12], can be used to enhance, mediate and enable specific reactions, providing another degree of freedom to modulate the properties of the nanoparticles.

The quest to engineer a biocompatible and environmentally friendly system with the highest quantum yield, for each of the half-reactions, is frequently reaching new peaks [7, 13]. However, so far, under mild working conditions, the performances are still inadequate. Moreover, the studies on half-reactions generally require the use of sacrificial additives that will extract one of the charge carriers from the nanoparticles [14]. These along with insufficient chemical stability of some of the proposed photocatalytic systems, limit their lifespan.

One of the current challenges is to expand this time duration, similar to what has been achieved for similar quantum materials, and yet for orthogonal use, in display applications [15]. The straightforward routes that have been examined and were found to increase the longevity of the nanoparticles are: (1) shell growth to protect them from undesired oxidation [6, 16]; (2) and/or coating the NCs with ligands or polymers that will facilitate the extraction of the unreacted charge carriers to the solution [17, 18].

A more intriguing solution, which future research needs to address, is the development of quantum systems capable of full water splitting, producing hydrogen and oxygen on two different catalytic sites. This may allow performing sacrificial

agents-free reactions while protecting the nanoparticles from non-desired degradation. A recently published study that showed the feasibility of this direction, utilized light excitation of semiconductor-metal hybrid nanorods functionalized with molecular catalysts (figure 1), to simultaneously produce hydrogen gas on the metal tip and oxygen gas through the surface coating [12, 19].

However, the yields are still relatively low and there is much to be done to improve them. Furthermore, efficient full water splitting will require careful handling and caution to prevent the highly exothermic reaction between hydrogen and oxygen from taking place before their separation.

Advances in science and technology to meet the challenges.

The market for hydrogen fuel is already out there, using oxygen and compressed hydrogen gas produced by steam-methane reforming to supply fuel for applications such as fuel cells for public transportation.

The progress in synthesis and surface engineering of NCs along with a better understanding of the processes involved in light-induced catalytic reactions in general and specifically in H₂ and O₂ generation will ultimately yield better photocatalysts. These will allow us to replace the currently polluting hydrogen production process to the desired renewable and environmentally friendly solar to fuel conversion.

In parallel, the natural technological advancements in the fuel cell vehicle field will further improve the know how to separate and store the hydrogen and oxygen gases and later control the reaction between them while benefiting from the released energy.

Concluding remarks. Colloidal quantum materials have come a long way since their first introduction. They are commercially available as light-emitting tagging agents and as components in displays, showing the path for their use in future applications. The inherent tunability of this unique class of NCs provides a large number of degrees of freedom that require long-lasting effort to reveal and understand the main principles governing their mechanism of action in each half-reaction. We also ought to address now the next challenges, which open a new exciting playground to explore, towards the commercialization of colloidal quantum material also as photocatalysts for solar to fuel conversion.

Acknowledgments

This work was supported by the Israel Science Foundation (Grant No. 1867/17). U B thanks the Alfred & Erica Larisch memorial chair.

2. Dye-sensitized solar cells

Gerrit Boschloo, Marina Freitag, Leif Hammarström, Erik M J Johansson, Jacinto Sá and Haining Tian

Department of Chemistry—Ångström Laboratory, Uppsala University, Box 523, SE-75120 Uppsala, Sweden

Status. In dye-sensitized solar cells (DSSCs), light is converted into electrical energy using light absorbing dyes, sensitizers, in a manner that has similarities to natural photosynthesis, but differs completely from conventional photovoltaics. Photoinduced electron transfer from the excited sensitizers to a mesoporous wide-bandgap semiconductor (usually TiO_2) is the first step in a rather complex working mechanism, see figure 2. This is followed by regeneration of the dye by the redox mediator, transport of electrons in mesoporous TiO_2 and redox mediators in the electrolyte and finally, reduction of the oxidized redox mediator at the counter electrode.

Ideally, dyes in the DSSC are adsorbed as a monolayer onto the mesoporous TiO_2 electrode. Initially, mostly ruthenium-based molecular sensitizers were used, but currently much research work is devoted to organic dyes, which can have higher extinction coefficients and avoid the use of rare metals.

Ever since the breakthrough work in 1991 [20], the triiodide/iodide (I_3^-/I^-) is the standard redox couple for DSSC. A favorable characteristic of this two-electron redox couple is the very slow recombination kinetics. A disadvantage is its multistep electron transfer mechanism that eventually leads to an internal voltage loss of about 0.5 V in the DSSC. In one-electron redox systems such as $\text{Co}^{\text{II/III}}(\text{bpy})_3$, $\text{Cu}^{\text{I/II}}(\text{tmbpy})_2$ and spiro-MeOTAD (a solid hole transporting material, HTM) such losses are avoided, but come at the cost of more rapid recombination reactions.

The DSSC is very versatile: they can have a wide variety of colors, depending of the dyes used, be opaque or semitransparent, and they can be made rigid or flexible. With a certified solar cell efficiency of about 12%, their performance does not match the best photovoltaic technologies under full sunlight conditions, but under low-light conditions that occur indoors their performance is unmatched [21]. Currently, commercial applications of DSSCs are in building integrated photovoltaics and in indoor power generation.

The general device structure of the DSSC is also very versatile, allowing for many variations in the research environment, as will be discussed below. Notably, the perovskite solar cell is directly derived from DSSC research (see section 4 of this paper).

Current and future challenges

Increase in efficiency. The DSSC photovoltage is given by the difference between the quasi-Fermi level of the semiconductor and the potential of the electrolyte redox couple. It is desirable to use redox couples with a potential close to that required to regenerate the dye.

However, regeneration then typically becomes slow, which may lead to dye-semiconductor charge recombination losses. Recombination between the oxidized form of the redox couple

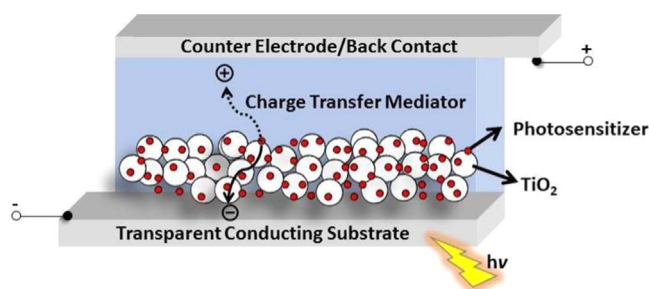


Figure 2. Configuration of a traditional dye-sensitized solar cell.

and electrons in the n-type semiconductor will also lower the Fermi level, and thus the photovoltage. A good illustration is a cell which used a $\text{Co}^{\text{II/III}}(\text{dtb})_3$ electrolyte, instead of I_3^-/I^- , to increase the photovoltage [22]. When triphenylamine was added as an intermediate electron donor between the dye and $\text{Co}^{\text{II/III}}(\text{dtb})_3$, both the photovoltage and photocurrent were increased, because of faster dye regeneration and thus suppressed recombination.

The photocurrent is the product of the light-harvesting efficiency (LHE), the charge injection efficiency (Φ_{inj}) and the charge collection efficiency (Φ_{col}). All three factors can reach high values (>90%) for the best performing cells. However, high LHE is usually limited to light with $\lambda < 700$ nm, and developing dyes with better absorption in the red and near-IR regions, while maintaining high Φ_{inj} and Φ_{col} , is an important challenge. In addition, the Φ_{col} can be lower than optimal at the maximum power point, because electrons accumulate in the conduction band under operating conditions, which increases recombination with the electrolyte.

Increase in long-term stability. Many factors affect the long-term stability of the DSSCs, for example electrolyte leakage, dye desorption and dye photodecomposition/photo-isomerization. To avoid electrolyte leakage, solvents with high boiling points, such as 3-methoxypropionitrile, polymer gel and ionic liquids, are therefore chosen. To date, ionic liquids have shown excellent improvements in the device stability [23]. However, the high viscosity of the ionic liquid limits the redox couple diffusion in the devices, resulting in a lower photocurrent compared to DSSCs with organic solvents. Dye desorption is mainly caused by basic additives in the electrolyte, such as tert-butylpyridine (TBP), which is normally used in the DSSCs to raise the semiconductor CB and improve photovoltage. Dye structure optimization by use of rigid units is a strategy to improve the photo-stability of the dyes.

Advances in science and technology to meet challenges.

The properties of a high-performing DSSC are intimately linked and it is difficult to optimize one without negative impact on the others. Consequently, there are several interconnected approaches to meet these challenges, and below we present a selection of these.

Increase in efficiency. Instead of molecular dyes, small semiconductor nanoparticles (quantum dots, QDs) with very

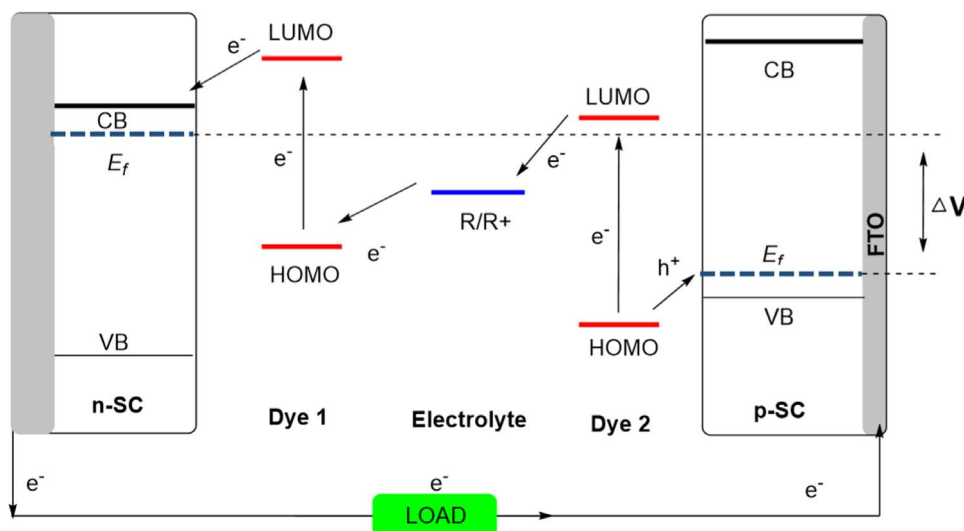


Figure 3. Schematic working principle of a tandem dye sensitized solar cell.

strong light absorption can be used [24]. This allows for the use of thinner TiO_2 films, which is useful for efficient charge collection with new redox couples and HTMs. The QDs used in DSSCs are usually made of CdS, CdSe and PbS and by changing the QD size it is possible to tune the light absorption edge from UV to near IR. Also, $\text{CH}_3\text{NH}_3\text{PbI}_3$ perovskite QDs were shown to work as light absorbers in DSSCs, which was the starting point for perovskite solar cells [25]. One problem with the most common QD DSSCs is the toxicity of the QD materials. However, progress in less toxic QDs have been made for example with AgS_2 QDs [26].

Plasmonic nanoparticles primarily from gold group metals have been utilized in the past as light absorbers enhancers but recently they were shown to act as direct light absorbers. X-ray spectroscopy suggested the formation of hot electrons, and these could be injected into accepting n-type materials, e.g. TiO_2 , which significantly prolonged their lifetime [27].

Simultaneous hot electron and hot hole injection into their respective acceptor layers was also demonstrated [28], paving the way to the development of direct plasmonic solar cells [29]. The true potential of this new type of solar cells remains incommensurate due to the poor understanding of the commanding steps involved, such as how many charges are created per photon, what is their energy distribution, what is the optimal operational voltage, etc.

A tandem DSSC (figure 3) consisting of a photocathode and a photoanode both sharing a redox couple broadens the light absorption wavelength range and adds photovoltage from the two halves. This gives a higher theoretical efficiency than a single photoelectrode device, and is in principle a straightforward way to overcome the Shockley–Queisser (S–Q) limit for a single bandgap. However, the state-of-the-art efficiency of a tandem device is still far away from that of a single n-type device due to the poor performance of its photocathode part [30]. The photocathode is typically based on mesoporous NiO, with rapid dye–NiO charge recombination as a main limiting factor [31], but other materials show worse or at best marginally improved DSSC performance.

Matching the optical absorption of both photoelectrodes by optimization of photosensitizers and improving the theoretical photovoltage by choosing suitable semiconductors are challenges of the tandem devices as well. A concept of solid state tandem DSSCs have also been proposed [32].

Increase in long-term stability. With hole transport materials (HTMs) instead of a liquid redox electrolyte the DSSCs can be a solid state device (ssDSSCs), which can also overcome electrolyte leakage issue. The reduction potential of HTMs should match the energy level of the photosensitizer and have intimate interaction with all photosensitizers in the devices. The HTM needs to efficiently fill the pores of the nano-porous electrode. Moreover, the HTMs should not compete with the photosensitizer for light absorption. Organic aryl derivatives have been successfully applied in ssDSSCs, rendering an efficiency of 7% [33].

The commonly used organic HTMs are limited in conductivity, stability and tunability. Coordination complexes were recently shown to combine benefits from organic small molecules and inorganic HTMs in terms of processing capability and charge conductivity. The efficient copper coordination complex-based HTMs, demonstrated a new concept [34] which gave the most efficient ssDSSC, with stable and record-breaking solar cell efficiencies of over 11% [35]. The next breakthrough requires the development of new charge-transport materials which overcome the remaining limitations, the high recombination rates, limited tunability and processability.

Concluding remarks. Application of DSSCs can be expected in several niches with different technical requirements, such as building integration and indoor applications. These may include semitransparent windows that reduce solar heating and at the same time generate electricity, and the wireless powering of ‘internet of things’. The modular and flexible DSSCs are well suited to meet these varying demands.

3. THz studies of nanomaterials for solar energy conversion

Rebecca L Milot¹, Laura M Herz², and Michael B Johnston²

¹Department of Physics, University of Warwick, Gibbet Hill Road, Coventry CV4 7AL, United Kingdom

²Department of Physics, University of Oxford, Clarendon Laboratory, Parks Road, Oxford OX1 3PU, United Kingdom

Status. A clear understanding of photogenerated charge dynamics in a material is key to its implementation in solar energy conversion devices such as solar cells and photocatalytic cells. However, for nanomaterials, even the most basic electrical properties such as electrical conductivity and mobility, which can be obtained by straightforward measurements in bulk samples, become extremely challenging to assess because of the difficulties associated with making electrical contacts to nanoparticles. Even if the contacts can be made, the contact-nanoparticle interface is likely to dominate the measurement rather than the intrinsic electrical properties of the nanoparticle itself.

Terahertz (THz) spectroscopy has emerged over the last few decades as a technique that can provide powerful insights into the electrical properties of materials [36]. As an optical technique, it avoids the need for physical contact with the sample, which is a huge advantage when dealing with ensembles of nanoparticles. A particular strength of the technique is that it may unravel the dynamics of photo-injected charge-carriers, which may, for example, involve charge separation or exciton formation, on a femtosecond to nanosecond time-scale. Such information is particularly valuable for designing solar energy conversion materials and devices.

THz studies of nanomaterials emerged at the turn of the millennium and focused on their fundamental properties, such as the size dependence of CdSe nanoparticle photoconductivity [37] and charge carrier trapping in Si nanoparticles [38]. To date a wide range of materials systems have been investigated, and here we give a brief introduction to the technique and summarize the status of the sub-field related to materials for energy conversion.

THz radiation refers to electromagnetic waves over a broad spectral range between microwave radiation and infrared light. It is usually defined as the frequency band from 100 GHz to 10 THz (wavenumber: 3–333 cm^{-1} , wavelength 3 mm–30 μm , photon energy 0.42–42 meV). This spectral range is fertile in features originating from fundamental charge processes in nanomaterials and includes the characteristic energy of electron correlations, such as excitons and plasmons, as well as spectral features associated with charge scattering.

While a range of techniques exist for spectroscopy in the THz regime [36], most studies of the electrical properties and charge dynamics of nanomaterials rely on the technique of optical-pump-THz-probe spectroscopy (OPTPS). In this technique, a femtosecond laser pulse is used to (i) generate a single-cycle THz pulse, (ii) optically excite a sample, and

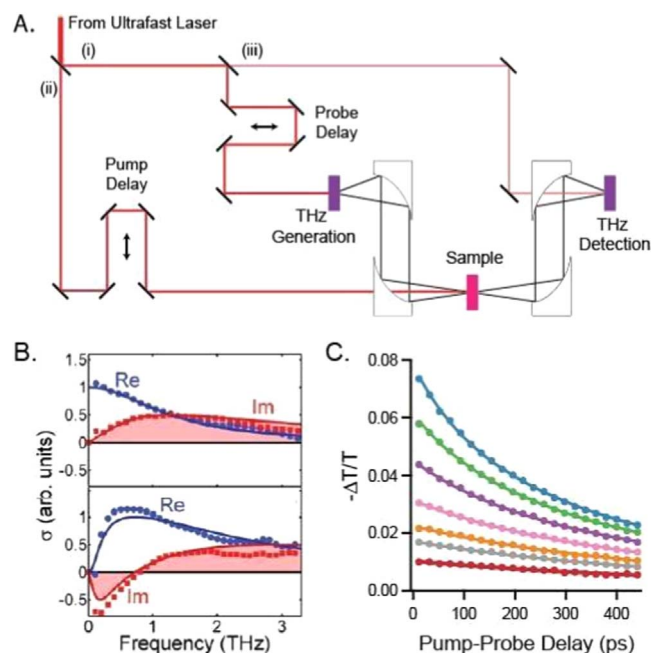


Figure 4. (A) OPTPS experimental setup. The output from an ultrafast laser is split into beams for (i) THz generation, (ii) sample photoexcitation, and (iii) THz detection. Both the optical pump and THz probe arms include a mechanical delay stage for time-resolved measurements. (B) Real (blue circles) and imaginary (red squares) components of the equilibrium conductivity σ of bulk GaAs (top) and GaAs nanowires (bottom) as reported in [39]. Solid lines represent fits to the Drude model (bulk) and surface plasmon model (nanowires). (C) Charge-carrier recombination dynamics of formamidinium tin-triiodide [40], a hybrid metal halide perovskite, measured following photoexcitation at 800 nm. The measured change in transmitted THz amplitude $-\Delta T/T$ is proportional to the product of the charge-carrier density and the charge-carrier mobility. The symbols represent experimental data, and the solid lines are fits to a simple recombination rate model to account for monomolecular, bimolecular, and Auger recombination [40, 41].

(iii) detect the THz pulse after it has been transmitted through or reflected from the sample (figure 4(A)). By changing the relative delay between the three pulses it is possible to record both the photoconductivity spectrum of the sample at a particular point in time after photoexcitation (figure 4(B)) and the photoconductivity dynamics as a function of the pump-probe delay time (figure 4(C)) [39].

The form of the photoconductivity spectrum over the THz band typically contains a wealth of information. As shown in figure 4(B), the spectral shape may allow Drude free carrier transport to be distinguished from a localized response. The plasmonic response of a semiconductor nanowire is clearly quite different from the Drude response of a bulk crystal.

OPTPS is having a growing impact in the field of energy conversion. One of the very first photophysical studies on then newly developed metal halide perovskite (MHP) solar cell materials was performed using OPTPS [41]. This study demonstrated accurate determination of charge mobilities and diffusion lengths for mesoporous MHP materials and helped lead to the realization that these materials were ideal for planar heterojunction solar cells. In addition, the technique

allowed charge recombination in the materials to be studied quantitatively, with both bimolecular and Auger constants obtained. Since this first report, OPTPS studies have remained at the forefront of MHP solar cell development and have revealed the potential of many novel materials, most recently including mixed two- and three-dimensional MHPs [42, 43].

Single crystal semiconductor nanowires are currently being implemented in solar cell devices and studied for photocatalysis applications. OPTPS has been used extensively to investigate and optimize these important materials. For example, surface charge recombination, which is very important in nanomaterials, was studied quantitatively with OPTPS. This study revealed an ultralow surface recombination velocity for InP nanowires which makes them highly suited to photovoltaic applications [44].

THz investigations of dye-sensitized metal oxide nanoparticles have provided detailed information about charge transport for applications including DSSCs and photoelectrochemical water oxidation cells.

Analyses of commonly used metal oxides nanoparticles such as TiO₂ revealed non-Drude photoconductivity that contrasts their Drude-like bulk response, suggesting localization of charge-carriers within particles [45]. Additionally, the timescale and efficiency of charge transfer from sensitizer molecules were found to be highly sensitive to the chemical composition and energetics of both the metal oxide and sensitizer [46, 47]. The dynamics can be further affected by the presence of an electrolyte [48], light-soaking [49] or the addition of a water-oxidation catalyst [50].

Current and future challenges. Arguably the largest source of controversy in the field at present concerns data processing and modeling. While THz photoconductivity spectra of thin-film and bulk samples are relatively straightforward to model and extract meaningful parameters, such as charge mobility, data obtained from nanomaterials pose a greater challenge.

A typical nanomaterial consists of an ensemble of nanoparticles within free space or a matrix of differing dielectric properties. The fact that, by definition, the length scale of a nanomaterial is much smaller than the $\sim 100 \mu\text{m}$ wavelength of the THz radiation is beneficial in that there is little scattering of the THz but does mean that the measured spectrum is that of the whole 'effective' material, rather than just the material making up the nanomaterial. There are several methods currently used to extract the intrinsic electrical properties of nanomaterials from the measured nanomaterial matrix, including effective medium theories (Bruggeman, Maxwell–Garnett), carrier transport models (plasmon, Drude–Smith), and computation solutions to Maxwell's equations, but little consensus on which is the most appropriate to use [51].

Another future challenge is the transfer of THz techniques from lab-based, fundamental science to useful industrial quality control for nanomaterials, ideally *in situ* as they are included in energy conversion devices. The noncontact nature of the technique is ideal for that application, but acquisition speed

reliability and signal to noise issues would need to be addressed before this goal can be met.

While most THz spectroscopy of nanomaterials has been conducted on thin films of material deposited on THz transmissive substrates (such as quartz), understanding the behavior of the nanomaterial while it is within a working device would be particularly powerful in the development of understanding of device operation.

Finally, there is growing interest in performing THz spectroscopy on individual, isolated nanoparticles, rather than an ensemble of nanoparticles. Scattering near field microscopy has been the lead technique in this area [52], with a new field of THz-STM now emerging [53]. At present these techniques face large challenges in terms of signal to noise ratio, and deconvolving the acquired THz spectrum from the instrument response, but have huge potential.

Advances in science and technology to meet challenges.

Current advances in computational methods and machine learning (ML) or artificial intelligence offer new opportunity for accurate and efficient parameter extraction from THz spectroscopic data. These developments may overcome some of the limitations of the simpler models currently used; however, these simpler models are likely to still be of great use in understanding fundamental properties of nanomaterials and the function in devices. Complex numerical models are unlikely to wholly replace well thought-out intuitive descriptions.

Technical advances are currently being made to enable THz spectroscopy to be performed in working devices. These advances have already enabled THz spectroscopy to be performed on dye sensitized solar cells whilst functioning [54]. Reflection based THz spectroscopy is also being exploited more to relax the constraints on suitable device substrates.

For realization of industrial quality control and to make single nanoparticle spectroscopy more applicable, improvements in THz technologies are still needed. Significant improvements in THz sources and detectors as well as the data acquisition electronics are needed to improve signal-to-noise levels. The advent of spintronic THz emitters and their continued development is a very positive sign in this direction [55].

Concluding remarks. Non-contact THz methods offer much to the field of nanomaterials for energy conversion. The intrinsic non-contact nature of this optical probe, the wealth of spectral data and ability to time-resolve charge-carrier dynamics are extremely powerful. Given this potential THz techniques are currently under-utilized in the field. Improving methods of extracting useful device data, such as charge mobility, along with further developments in THz technologies will lead to wider usage and ultimately uptake in quality control of industrially-produced energy conversion devices based on nanomaterials.

4. Perovskite solar cells

Ioannis Spanopoulos, Weijun Ke and Mercuri G Kanatzidis

Department of Chemistry, Northwestern University, Evanston, IL 60208, United States of America

Status. Organic–inorganic hybrid perovskites with a general formula of AMX_3 ($A = Cs^+$, $CH_3NH_3^+$ (MA), $HC(NH_2)_2^+$ (FA); $M = Ge^{2+}$, Sn^{2+} , Pb^{2+} ; $X = Cl^-$, Br^- , I^-) [56], exhibit excellent optical and electrical properties thus enabling the fabrication of high performance solar cell devices [57–60]. To date, the record power conversion efficiency (PCE) values are above 25% for single-junction perovskite solar cells and outperform those of multicrystalline silicon (23.3%), $Cu(In,Ga)(Se,S)_2$ (23.3%), and CdTe (22.1%) [61]. Higher efficiency values can be achieved by the assembly of tandem modules. The tandem devices consist of two or more junctions where the higher energy photons can be absorbed by the top absorber layer with higher band gap, and lower-energy photons will be absorbed by the bottom, lower band gap, light absorbing material [62]. In this way a wider range of the solar spectrum will be absorbed and exploited. Characteristic tandem devices are based on mixed Pb/Sn perovskite materials [63, 64], perovskite/silicon [65], and perovskite/ $Cu(In,Ga)(Se,S)_2$ [66]. So far, the most efficient solar cell devices are based on Pb perovskites, e.g. $Cs_xFA_{1-x-y}MA_yPbI_{3-z}Br_z$ [67, 68]. The corresponding very high efficiency values stem from many strategies that have been developed and implemented (figure 5). These include the use of new perovskite materials (2D, 1D, 2D/3D) [69], additives [70], ingenious device structures [71], passivation [72], and optimization of film assembly [73]. These exceptional PCE values of perovskite solar cells, depict the huge potential of these materials in replacing current photovoltaic silicon based technologies, where a less suitable solar absorber material (Si is an indirect bandgap semiconductor) dominates the market.

Current and future challenges. Despite the very promising device performance values there is still a long way to cover until the extensive commercialization of those materials. There are two major bottlenecks that must be overcome before a new era in semiconductor devices can commence. The first one is their composition of toxic elements (e.g. Pb), which is already addressed and accounted for (see below) and the second and most important one is their environmental stability (air, heat, and light) under an extensive time period (>20 years).

The 3D halide lead iodide perovskite structure has been extensively studied and apparently its unique structural characteristics render it a highly competent solar cell absorber [74]. Equally prominent is the work on 2D based hybrid perovskite materials [75] with a recorded PCE value up to 18.2% [76]. Similarly 2D/3D solar cell devices based on hybrid perovskite materials exhibit a recorded PCE value up to 22%, maintaining at the same time 90% of their efficiency during photovoltaic operation for 1000 h in humid air under

simulated sunlight [77]. All of these studies are based on Pb perovskites, and the recorded environmental stability tests provide limited comprehensive information for their heat, air and light stability.

In the case of fully Pb based perovskites, recent studies shed light on the life-cycle environmental impact of assembled perovskite/silicon tandem modules, containing lead based hybrid halide perovskites as the upper layer. The results revealed that the emitted lead contributes only 0.27% or less to the total freshwater ecotoxicity and human toxicity, as compared to the other solar module components [78], because the perovskite film thickness is very low <500 nm [65]. Nonetheless, the Pb toxicity concern can be addressed by replacing Pb^{2+} by Sn^{2+} , either in part or in total [79]. We were the first to report [80] and exploit the fact that the energy band gaps of the mixed Pb/Sn compounds $MAPb_xSn_{1-x}I_3$ do not follow a linear trend (Vegard's law) in between the two extremes of 1.55 and 1.35 eV ($MAPbI_3$ and $MASnI_3$) respectively, but have narrower bandgap (<1.3 eV), thus extending the light absorption into the near-infrared (~1050 nm) [64]. Tin based perovskites are even more efficient in solar-energy absorption because of their reduced band gap and lower carrier effective masses [81, 82]. However Sn^{2+} based perovskite materials are not air stable, as Sn^{2+} oxidizes rapidly to Sn^{4+} , leading to material degradation [83]. The complexity of these issues dictates the need for even better materials, or new strategies to improve the properties of the current Pb and Sn based ones.

Advances in science and technology to meet challenge.

There are many approaches to improve the environmental stability of the current based technologies. They focus on two different directions. The first is the protection of the assembled device by encapsulation, using various methods such as thermoplastic sealants and thermally or UV curable epoxys [84, 85]. In this way the stability of the corresponding device can be improved substantially, by preventing moisture and oxygen to reach the perovskite light absorbing layer. The efficiency of these methods depends on the sufficient protection of the sealant which must be also heat and light stable, passing the established stability criteria such as ISOS-D-3 (damp heat), and ISOS-L-3 which require not only high levels of humidity (RH: 50%–85%), but also high temperatures (65°C–85°C) and 1 sun illumination (AM 1.5G) [86, 87].

The second direction involves the development of new type of perovskite materials (3D, 2D, 1D) with structural characteristics that can enhance their inherent air, heat and light stability. Passarelli *et al* used bulky polyaromatic linkers such as pyrene-o-propylamine for the synthesis of 2D perovskite materials with chemical formula $(R-NH_3)_2PbI_4$, where the assembled films exhibited superior water stability, as they maintained their crystallinity after immersion into liquid water for up to 5 min [88]. This work provided proof that hybrid halide perovskites can indeed become water stable. In this case the band gap of the resulting material was not optimum for the assembly of single junction solar cells

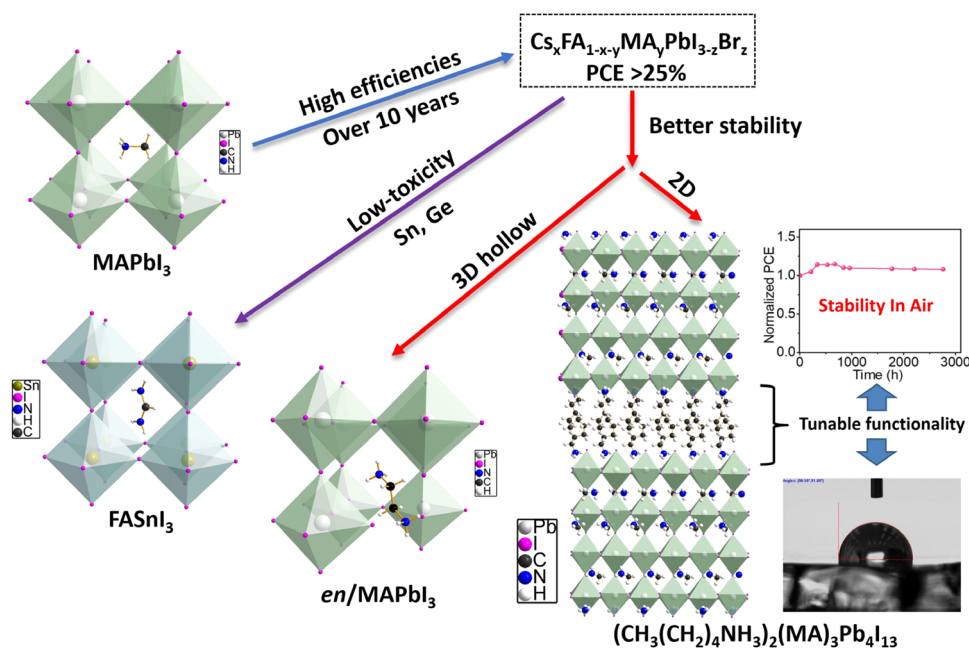


Figure 5. Evolution of perovskite materials for the assembly of high efficiency (PCE) solar cells, and synthetic methodologies for addressing toxicity and environmental stability deficiency issues.

(~ 2.3 eV), but it could be suitable for the assembly of air stable tandem devices providing sufficient protection from moisture. In terms of acquisition of stable Sn based perovskites, we reported recently a novel strategy which included the use of a small organic molecule, ethylenediamine (*en*), as an additive during the synthesis of 3D hybrid halide perovskites, leading to the formation of the so called ‘hollow’ 3D perovskites. The synthesized materials exhibited a substantial increase of the air stability by two orders of magnitude as compared to the pristine 3D analog MASnI_3 , e.g. in the case of $(\text{MA})_{0.6}(\text{en})_{0.4}(\text{Sn})_{0.72}(\text{I})_{2.84}$ compound [89]. The corresponding benefits spanned beyond stability as it also allowed the fine tuning of the band gap from 1.1 eV for the pristine material to 1.51 eV for the 40% *en* based one, value which lays in the optimum range for maximizing the corresponding solar cell device efficiency.

In our group we designed a series of experiments to evaluate the inherent air, heat and light stability of three different families of 2D hybrid perovskites, $(\text{BA})_2(\text{MA})_{n-1}\text{Pb}_n\text{I}_{3n+1}$ ($n = 1-5$, $\text{BA} = \text{CH}_3(\text{CH}_2)_3\text{NH}_3^+$), $(\text{PA})_2(\text{MA})_{n-1}\text{Pb}_n\text{I}_{3n+1}$ ($n = 1-5$, $\text{PA} = \text{CH}_3(\text{CH}_2)_4\text{NH}_3^+$) and $(\text{HA})_2(\text{MA})_{n-1}\text{Pb}_n\text{I}_{3n+1}$ ($n = 1-4$, $\text{HA} = \text{CH}_3(\text{CH}_2)_5\text{NH}_3^+$), including perovskite films cast on various substrates. One of the most important finding is that if the films are efficiently protected from O_2 and moisture through a suitable sealant assembly, the heat (e.g. 90 d continuously at 100 °C) and light stability increases drastically, validating that these materials are indeed inherently heat and

light stable [90]. These conclusions clearly indicate that a functional, efficient and stable perovskite solar cell can be materialized if a suitable sealing protection is achieved.

Concluding remarks. The rapid advances in the field of perovskite solar cells, clearly indicate that both highly efficient and environmentally stable perovskite devices can be assembled. This is achieved through suitable materials design and device engineering. Since 2D hybrid halide perovskites are inherently heat and light stable, in the absence of moisture, then in our opinion, one of the remaining issues to be investigated is the sealing procedure of the corresponding solar cell devices. This includes evaluation of the adhesion performance, and stability of the sealant materials, under air, heat and light, for a considerable amount of time, and under extreme conditions (e.g. 100 °C, RH = 80%, 1 sun illumination). These measurements would provide valuable information to the industry and the scientific community for the extend that these materials can be accounted for, before degradation.

Acknowledgments

This work was supported by ONR Grant N00014-20-1-2725.

5. Multiscale computational methods for generating accurate nanoscale structures in OPV materials

Kevin L Kohlstedt and George C Schatz

Department of Chemistry, Northwestern University, Evanston, IL, United States of America

Status. The intense rise of organic photovoltaic (OPV) device efficiency during the beginning of the 21st century is one of the major achievements of materials chemistry. Although gains in efficiency have not been steady, as the picture of the device active layer has become clearer, synthetic strategies have evolved to tune details of film structure toward finer and finer control. Underpinning that effort, computational modeling of OPV films has been critical in elucidating the molecular details of the nanoscale domains in the film and connecting rational design strategies to the performance of the device. While much effort of the past quarter century has gone into developing models that predict structure–property relationships at the molecular level, predicting nanoscale properties of photovoltaic devices from single-molecule calculations has been a challenge. In principle, all of the electronic properties and intermolecular packings are encoded in monomer or dimer level models, yet, device-level measurements, such as film mobility have been bedeviling for computational models to accurately predict. Recently, computational efforts have begun to investigate the nanoscale features of the OPV films based on the intermolecular interactions and nanostructure geometries.

Existing computational models for predicting OPV device performance are mainly based on two types of approaches. The first approach consists of self-consistent continuum models in which optoelectronic information of the organic materials is parametrized either from electronic structure (DFT or wavefunction-based) calculations of varying levels of detail or spectroscopic measurements. The accuracy of these models has improved considerably over the last few years due to a better description of bimolecular recombination kinetics at the domain interfaces, as well as carrier mobilities in the OPV films [91, 92]. The second approach is the use of thermodynamic atomistic modeling (molecular dynamics, Monte Carlo) for the prediction of the solid-state film microstructure that can be then used for direct calculation of charge generation and transport of the material [93]. The utility of the models depends on whether one can sample the necessary thermodynamic states of the organic film. Glassy dynamics of the polymer, semi-crystalline molecular domains, tractability of simulations at the necessary length and time scales, and determination of realistic force field parameters make these simulations difficult to broadly adopt. Ideally, these two approaches could be used in concert, such that detailed morphology information would lead to better quantum dynamics predictions of the excited state kinetics. Yet, for all the above reasons, linking the two approaches has been the exception rather than the rule.

One solution to link-up *both* the continuum and atomistic models, as well as increase the breadth of the organic materials designed for better forming OPV devices, is the use of data informatics. Data models, without any physical foundation, rely

on correlations of large datasets to relate molecular properties to device performance characteristics like PCE and mobility. Although the lack of physical insight from data correlated models make them controversial, the utility of them is entirely based on the length scales of the properties put into the datasets. ML methods do not learn physics, yet one can still test physical principles against the structure–property relationships found from the data [94]. As the use of artificial neural networks, nonlinear regression, and clustering algorithms becomes more widespread it is critical that multiscale physical properties be included as device performance is more directly correlated to nanoscale morphology than to single-molecule valence shell structure. In this roadmap, we detail the challenges and current efforts that are leading towards gains in improvements for molecular models and the data-driven methods built from them.

Current and future challenges. A current challenge in OPV device modeling is how to generate reasonable structural information at the heterojunction boundary. As small molecule acceptors have transitioned from fullerenes towards large quadrupolar dye molecules, this challenge has become even thornier now due to the dye molecules having multiple crystalline packings and strong dispersion interactions with the donor polymers. This has made mean-field models insufficient to systematically capture the average enthalpic interaction at the interface between the donor–acceptor domains. Recent coarse-grained molecular force fields are showing promise to generate detailed interfacial information, although getting proper π – π stacking distances continues to be a challenge due to the sphericity of the coarse-grained beads over-estimating the distance normal to the π -plane [95]. Lack of fidelity of π -stacking make it difficult to predict charge transport properties from structures generated from coarse-grained models, yet if they are consistent in their overestimation that can be corrected in the mapping back to atomic coordinates [96].

A second challenge relates to translating the thermal disorder from the structural predictions into the carrier transport calculations. For morphologies that include a large amount of crystalline and semi-crystalline domains, Gaussian disorder models have not been uniformly successful to describe the fragility of the transport networks due to anharmonicity and correlated disorder in and between the crystalline domains. Network methodologies that include dynamic disorder offer a solution that tracks the correlated disorder in the predicted structures [97]. Yet, those structures generated from molecular dynamics do not account for the excited state geometries, including anharmonicity, especially for the flexible non-fullerene acceptors like A-D-A molecular triads [98]. Overcoming both of those issues will allow structural predictions from ground state thermodynamic simulations to translate to better predictions of the charge mobilities.

As the computational efforts move forward, a major outstanding challenge will be to successfully implement the multiscale physics of charge transport into ML algorithms. Going beyond single molecule inputs into the training sets will be vital for correlating molecular topologies to film mobility and photo-current efficiency of the OPV device. Generating

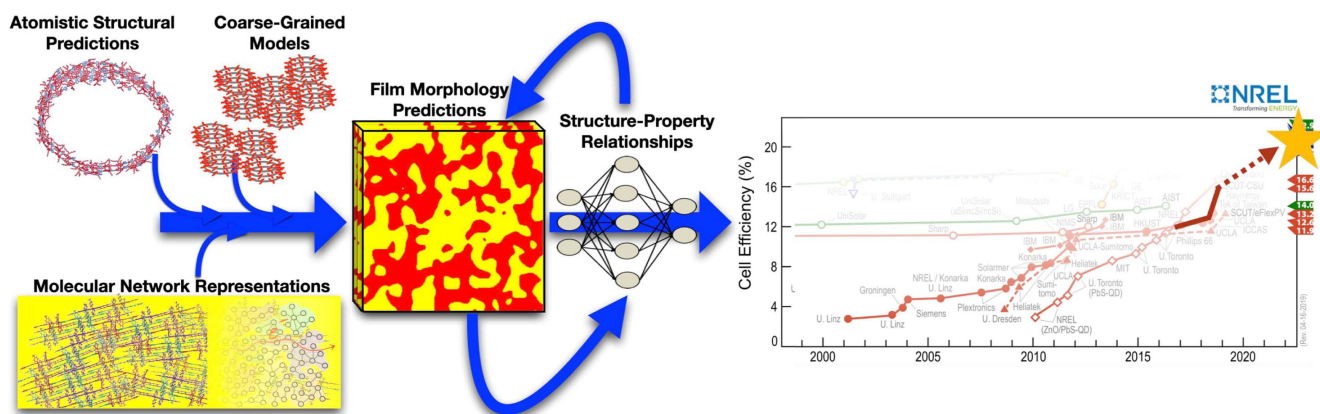


Figure 6. Integration of multiscale computational efforts for detailed nanoscale BHJ morphology prediction. Both small molecules and polymers can utilize the four computational frameworks highlighted in this roadmap: atomistic structural predictions, coarse-grained models, molecular network representations, and structure–property relationships (ML, miscibility relationships, processability data). The historical PV device efficiency data were taken from NREL published ‘Best Research-Cell Efficiency’ [100].

structured datasets that include the organizational information of the heterojunction is a challenge both for understanding the structure–property relationships that have led to the recent improvement in devices with 16% photo-current efficiency and for more quickly screening molecular candidates to push efficiencies towards 20% efficiency (figure 6) [99].

Advances in science and technology to meet challenges. In order to generate thermodynamically relevant structures, larger, multicomponent (donor and acceptor) systems need to be modeled. Further development of coarse-grained force fields will be key to modeling the size of the systems necessary, especially to reach the timescales needed to relax polymeric structures. Further acceleration of molecular dynamics on high-throughput clusters like graphics processing units will be important to generate the scale of structural data needed for both transport models and ML training sets.

Although mean-field models currently lack the correct enthalpic interactions between the donor–acceptor domains, large scale coarse-grained molecular dynamics could allow calculations of structural factors that lead to corrections in the average interaction energy χ , such as virial coefficients that account for structural correlations. Temperature dependent miscibility measurements via x-ray microscopy are becoming more common on donor–acceptor films that include crystalline domains and can provide an experimental check on the mean-field predictions [101]. Mean-field miscibility predictions offer great promise as a dataset that encodes the phase behavior (binodal curve) and percolation ratio, while still being based on microscopic structural details. Once a large dataset, $>10^2$ pairs, has been established using corrected mean-field calculations and tested against miscibility measurements, ML will be an effective tool to predict transport properties of unknown pairs of donor/acceptor molecules. Where χ predictions fail, atomistic aggregation predictions can provide detailed domain structural information and domain interfacial energy [102].

Another direction with great promise for providing molecular data for OPV databases that includes structural information is electronic coupled networks. Charge transport networks offer a compact way to store carrier percolation information based on structural predictions via molecular dynamics, Monte Carlo, or even film micrographs. Network analysis, more generally, has been a key methodology to condense a large set of structural degrees of freedom, showing how molecular order relates to the general optical properties of the material [103]. For instance, as design of molecular systems with tunable excited state properties based on the structural details of the aggregate becomes more common in nonlinear optics, aggregation-induced fluorescence emission, and near-IR biological imaging, network models will be in a strong position to provide structure–property relationships from complex organized systems [104].

Concluding remarks. Structural prediction of molecular morphologies in OPVs remains an outstanding issue in device modeling. Although much of the foundational optoelectronic principles have been learned over the past couple of decades, it remains largely unsolved to predict the charge transport capabilities of a newly conceived OPV donor/acceptor. As the computational efforts begin to move from generating structure–property relationships to organic semiconductor design, high-fidelity coarse-grained models are going to be necessary to generate the detailed thermodynamic structures. Network models can then pull out organizational trends and reduce the dimensionality of the data to input into training sets to build the material prediction capabilities of ML methods.

Acknowledgments

The authors acknowledge the support by the Center for Light Energy Activated Redox Processes (LEAP) Energy Frontier Research Center under the award DE-SC0001059.

6. Solar-driven water splitting

Nathan S Lewis

Division of Chemistry and Chemical Engineering, and Beckman Institute 210 Noyes Laboratory, 127-72, California Institute of Technology, Pasadena, California 91125, United States

E-mail: nslewis@caltech.edu

Solar-driven water splitting requires a synergistic combination of light absorbers and electrocatalysts, as well as processes to effect product separation [105]. These functions can be achieved as separate process steps, such as by use of a photovoltaic cell coupled to an electrolyzer, or in an integrated system that evolves separate streams of $\text{H}_2(\text{g})$ and $\text{O}_2(\text{g})$ with only water and sunlight as the inputs [106]. The discrete component approach and integrated systems approach have some mutual commonality but also entail substantial differences in performance, materials, and design strategy. Fully integrated systems are the focus of this status report.

Status. Stand-alone fully integrated solar-driven water splitting systems are relatively rare, with none existing commercially or at the large-scale demonstration stage. In laboratory demonstrations, however, the efficiencies of such systems have increased markedly in the past few years [107]. Solar-to-hydrogen efficiencies in excess of 10% have been demonstrated in systems that produce safe, separate streams of $\text{H}_2(\text{g})$ and $\text{O}_2(\text{g})$ [108], with efficiencies as high as 19% reported for systems that co-evolve stoichiometric mixtures of $\text{H}_2(\text{g})$ and $\text{O}_2(\text{g})$ [109]. To be considered for eventual commercialization, four system-level criteria must be met simultaneously: high efficiency, stability, safety, and the potential for low-cost/scalable manufacturing. At present, no demonstrated system meets all of these criteria simultaneously. Long-term stability of efficient solar light absorbers in contact with a liquid electrolyte is a long-standing challenge, as is the stability of active, earth-abundant electrocatalysts for the redox reactions needed to sustainably make fuel.

Systems with the highest efficiencies are not scalable and/or not stable. Chemical processes (membranes or separators) and/or physical mechanisms (gas or liquid-based separations) that maintain ample separation of the products are currently not scalable, cost-effective, energy efficient and stable. Additional challenges arise when all of the components in a fully integrated system must function under a mutually common set of reaction conditions. Nevertheless, integrated systems have substantial potential advantages in simplicity, cost, and performance relative to discrete photovoltaic/electrolyzer assemblies, making integrated systems attractive targets for exploration, proof-of-concept, and development of components, devices, and engineering designs.

Current and future challenges

Electrocatalysts. The most active electrocatalysts in acidic media for oxidation of water to $\text{O}_2(\text{g})$ contain precious metals such as Ru and Ir [110]. The scarcity of these elements would preclude scale-up of such systems, in their current form, to meet current global fuel demand. In acidic media, Pt is the most active electrocatalyst for reduction of protons to $\text{H}_2(\text{g})$. Challenges involve finding alternative active electrocatalysts that are also stable under operating conditions. For water oxidation in acidic media, the search is for a non-precious noble metal, which is arguably an oxymoron. A material needs to have sufficient covalency that the otherwise ionic electrocatalyst component of the material is rendered insoluble in acid and is not leached from the structure, while also exhibiting a high degree of activity at low overpotentials for the highly kinetically demanding four-electron oxidation of two water molecules to form $\text{O}_2(\text{g})$ [111]. Earth-abundant transition-metal sulfide-based [112] and/or phosphide-based [113] electrocatalysts have been developed for evolution of $\text{H}_2(\text{g})$ under acidic conditions. Although these materials are stable for days of operation in the laboratory, long-term stability under operating conditions, including day/night cycling of the electrocatalyst under operating potentials, is not yet demonstrated.

In alkaline media, stable earth-abundant electrocatalysts based on Ni–Mo and related alloys, in which the Mo stabilizes the active Ni electrocatalyst site, are used commercially in alkaline electrolyzers for $\text{H}_2(\text{g})$ evolution [114]. Moderately low (280–350 mV) overpotential earth-abundant electrocatalysts based on Fe–Ni oxyhydroxides and related compounds catalyze water oxidation to $\text{O}_2(\text{g})$ in alkaline media, and are stable for extended time periods [110]. Unlike the situation in acidic media, in which the limited suite of stable earth-abundant $\text{O}_2(\text{g})$ -evolving electrocatalysts have very high overpotentials, in alkaline media little performance gain in an integrated system could be achieved by lowering the overpotentials of electrocatalysts, relative to use of currently available materials [115]. Hence the challenges in alkaline media primarily relate to effective integration of the available electrocatalysts into a fully functional system. Optical obscuration of light absorbers by the electrocatalysts needs to be managed and minimized [116]; electrocatalysts that develop porosity during operation can provide pathways for electrolyte to corrode the underlying light absorber; bubble formation needs to be controlled and beneficially exploited to enhance local mass transport without deleterious electrochemical and/or optical effects on operation [117]; and long-term stability under light/dark cycling conditions remains a concern.

At near-neutral pH, suitable electrocatalyst stability and activity remain to be demonstrated. Operation of a system at near-neutral pH entails either compromising safety by co-evolving stoichiometric mixtures of $\text{H}_2(\text{g})$ and $\text{O}_2(\text{g})$, or requires a membrane that leads to electro dialysis of the electrolyte and ultimately precludes efficient operation of the system [118]. The fundamental challenge arises from the use of an electromotive force in artificial photosynthetic systems, as opposed to the protomotive force used in natural

photosynthesis. In the former, for sustainable operation of a system, the pH gradient that is an inevitable consequence of trans-membrane electron transfer must be neutralized, with concomitant loss of the associated chemical potential. In contrast, natural photosynthesis beneficially utilizes the pH gradient produced by the protomotive force to actively facilitate cross-membrane transport of protons and stores energy in the reductive parts of the system by making and breaking chemical bonds.

Passive, scalable and energy-efficient methods of overcoming this fundamental challenge remain a roadblock at the system level under near-neutral pH operating conditions regardless of whether active, stable electrocatalyst components and materials for water-splitting are developed.

Light absorbers. Optimal light absorbers combine effective absorption of the solar spectrum with stability under operating conditions. No photoanode is thermodynamically stable in water under illumination [119], and hence kinetic stability must be exploited. Although oxides are generally stable under illumination in the laboratory, these materials all have a very low-lying valence band that is O 2p in character. It is not known whether stability is even possible in concept for an oxide-based material in which the band gap is decreased by substantially raising the energy of the valence band towards the formal potential for water oxidation. Photoelectrodes have been stabilized by use of protection layers, such as amorphous TiO₂, that conduct holes and prevent corrosive contact with the electrolyte [120]. The long-term failure mechanism of such systems, as well as methods to mitigate pitting-induced corrosion due to defects in the coating and/or local passivation approaches to extend operational lifetimes from weeks to decades, remain to be elucidated and demonstrated. Relative to stabilization of photoanodes, stabilization of photocathodes presents additional challenges due to the difference in failure mechanisms and consequently the differences in strategies required for development of suitable protection layers. Moreover, relative to the oxidative self-cleaning behavior of anodes, cathodes exhibit increased susceptibility to poisoning due to plating of metal impurities, and thus have more stringent requirements on purity of the input water stream.

Performance degradation can also occur due to pinholes or defects in the protective coating, producing shunts when plated metal impurities form local Schottky barriers or ohmic contacts with the underlying semiconductor.

Advances in science and technology to meet challenges. The key advances in science and technology to meet the

above challenges are all associated with materials by design. The desired properties and characteristics of the catalysts, separators, and light absorbers are all known and readily quantified, whereas discovery and identification of materials that have the specified combination of these chemical and physical attributes remain lacking at present. For each of the critical components of an integrated solar-driven water-splitting system, a combination of experiment, theory, and high-throughput data-driven methods will be needed to make rapid progress. The required properties must moreover be exhibited synergistically in an integrated system that operates under a mutually common set of conditions for every component in the system. Maintaining optionality is important because the first demonstrated integrated system is unlikely to be the final deployed system, and a variety of approaches should be pursued in parallel to optimize the chances of success.

Concluding remarks. Only three biogeochemical cycles have adequate mass flux at the Earth's surface to provide sustainable fuels for global civilization: the water/H₂ cycle; the N₂/NH₃ reduced nitrogen cycle, and the CO₂/C_xH_y reduced carbon cycle. Thermochemical catalysts are already known and implemented at scale for the efficient mutual interconversion of these fuels. Out of the three possibilities, water is the only substrate that is a liquid at room temperature that also can be used to produce fuel. Consequently water provides the only species with adequate mass flux from the atmosphere that is capable of matching and efficiently directly utilizing the incident solar photon flux in conjunction with a scalable liquid-phase electrochemical reactor. Moreover, an energy-intensive product separation process is minimized when the reaction products are gases. Hence addressing the science and materials development challenges associated with a direct solar-driven water splitting system is necessary, and sufficient, to enable a commercially viable, sustainable technology for the direct production of fuels from sunlight.

Acknowledgments

The Department of Energy, Office of Basic Energy Sciences, grant DE-FG02-03ER15483, and the Department of Energy, Office of Science, through the Joint Center for Artificial Photosynthesis, award SC-0004993, are acknowledged for support that made preparation of this manuscript possible.

7. Surface-bound molecular assemblies on nanostructured electrodes for solar fuel generation

Tom Meyer

University of North Carolina at Chapel Hill, Department of Chemistry, United States of America

Status. In solar energy conversion, the Sun is a wonderful, but limited resource because it is available globally for only six hours a day. A way to incorporate it more broadly into photovoltaic energy schemes arises from solar water splitting into H₂ or O₂ or by the reduction of CO₂ into solar fuels. We describe here the integration of water oxidation, and water or CO₂ reduction, at separate semiconductor electrodes in photoelectrochemical cells, as a way to capture solar energy and store it as a translational energy source. Experiments in this area began in the 1970s following a paper by Honda and Fujishima [121] who showed that UV excitation of nanoparticle TiO₂ films in an electrochemical cell with a separate Pt electrode gave O₂ and H₂ with an applied bias of 0.2 V. Their observation opened a new door to solar energy conversion based on using the energy of the Sun for water oxidation and water or CO₂ reduction at separate photoelectrodes in semiconductor solar cells.

Current and future challenges. Significant challenges existed in this area from the beginning. In the 1970s there were no molecular catalysts for water oxidation, no systematics for binding molecules to surfaces, and no basis for creating stable surface molecular structures. At UNC we demonstrated that excitation of the metal-to-ligand charge transfer excited state of [Ru(bpy)₃]²⁺ (bpy is 2,2'-bipyridine) with the added bipyridinium dication methyl viologen, MV²⁺, in acidic solutions, gave [Ru(bpy)₃]³⁺ and MV⁺ as transient products with the two separately capable of water oxidation and reduction [122]. We also demonstrated the first catalyst for water oxidation, cis,cis-[(bpy)₂](H₂O)RuORu(H₂O)(bpy)₂]⁴⁺ [123], and the importance of proton-coupled electron transfer in oxidative activation [124]. The first reductive catalysts for CO₂ reduction, including examples from our own group [125–128], were identified, as were procedures for the preparation of molecular assemblies by ligand bridging [129, 130] and electropolymerization [131] along with the evolution of procedures for the preparation of DSSCs [132].

This approach to solar fuels led to the dye-sensitized photoelectrosynthesis cell (DSPEC) [133–135]. The latter utilizes separate electrodes and ~10–20 nm nanoparticulate films for the two half reactions. It exploits chemical synthesis for the preparation and modification of chromophores and catalysts. The key semiconductor for *photoanodes* is TiO₂ [132]. It has a band gap of ~3.2 eV and a conduction band potential of 0.2 V versus NHE at pH 0. Ultrafast kinetic studies have shown that excitation of a surface-bound Ru(II) bpy dye, with an excitation maximum at 450 nm, leads to unit injection [136]. As a way to mitigate against back electron transfer after injection, a thin, multi-nanometer-thick layer of

TiO₂ is used as the outer layer in core/shell structured electrodes with SnO₂ as the inner electrode [137]. The core-shell structure exploits the 0.4 V decrease in potential at SnO₂ to minimize back electron transfer although with loss of external driving force at the electrode. In forming assembly structures on electrode surfaces, addition of the chromophore was followed by a surface-bound catalyst [138], although films have been investigated with the catalyst added externally in a separate external film [139].

In *photocathode* applications, the semiconductor choice is also very limited. The valence band potential at NiO is desirable energetically at ~0.9 V versus NHE [140] but injection efficiencies are low because of rapid back electron transfer at the electrode surface [141, 142]. Additional electrodes have also been investigated, including nanostructured tin-doped indium oxide (nanoITO) [143], p-type Si [144], and p/n junction Si/GaN nanowire arrays [145]. Si/GaN is promising but expensive to obtain at scales appropriate for preparing solar cells. P-type Si nanowire arrays have been used for water-reduction photocathodes, but with relatively low efficiencies [144].

Significant progress has also been made on electrode design. On surface binding, for both water splitting and CO₂ reduction, stable surface structures form by using phosphate-derivatized chromophores and catalysts on oxide surfaces [135]. After forming surface structures, the surfaces are stabilized by addition of ~1 nm overlayers of metal oxides by atomic layer deposition (ALD) [146]. More complex structures can also be prepared as overlayers following addition of a thin layer of metal oxide by ALD for further surface binding [139].

As a way to vary light absorptivity and excited state energetics, a variety of chromophores have been explored—polypyridyl complexes, porphyrins, and a variety of organic dyes [135, 147]. Water oxidation catalysis has been dominated by surface-bound metal polypyridyl complexes [138, 148]. Our recent research has focused on a Ru(II) polypyridyl catalyst [149], first prepared by the Sun group [150], with a redox potential for a reactive Ru(V/IV) couple that lies near the potential for the O₂/H₂O couple for water oxidation. In recent experiments, with long-chain organic links on electrode surfaces, Ru(II)bpy photoanodes have been prepared that have extended photocurrents of ~1 mA cm⁻² over a period of hours [151].

For *photocathodes* progress has been made with NiO as the electrode by modification of the electrode surface, but typically, surface kinetics are inefficient even for complex assemblies. Nonetheless, important results with catalysts for both water oxidation and CO₂ reduction have been reported [152]. On GaN, relatively high efficiency, ~1 mA cm⁻² photocurrent efficiencies [145] have been observed for extended periods but, as noted above, with difficulties in electrode preparation. Less efficient Si-based nanowire electrodes, that are relatively stable, have also been explored and used with added chromophore-catalyst assemblies for water reduction to hydrogen [144].

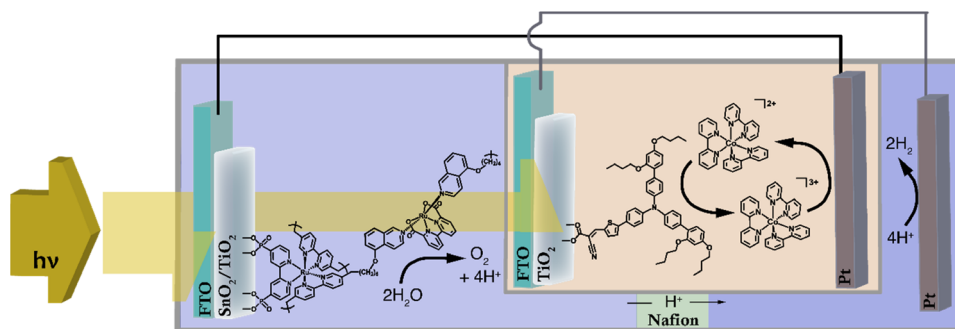


Figure 7. Schematic diagram for an electro-assembled core-shell based DSPEC wired in series with a dye-sensitized solar cell that used the D35 dye and a $[\text{Co}(\text{bpy})_3]^{3+/2+}$ mediator. Reprinted with permission from [153]. Copyright (2016) American Chemical Society.

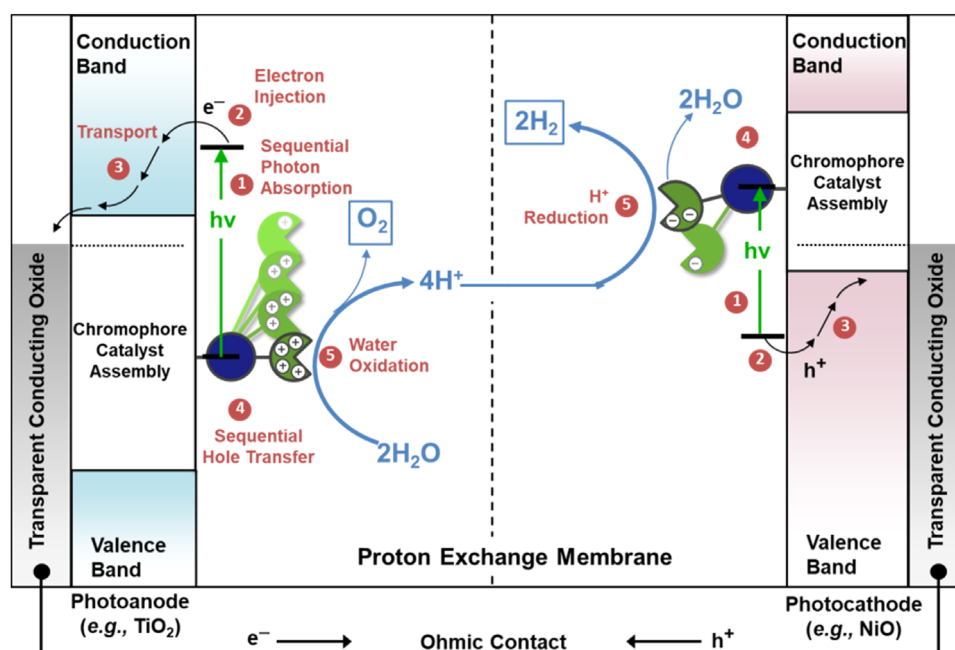


Figure 8. Schematic diagram of a DSPEC for solar-driven H_2O splitting into H_2 and O_2 . Reprinted with permission from [135]. Copyright (2016) American Chemical Society.

Applications. A variety of approaches to energy conversion have been explored based on DSPEC electrodes. **Assisted water splitting**—To overcome the required redox potential disadvantage in using TiO_2 -based photoanodes, a tandem device has been prepared that integrates an O_2 -evolving photoanode in series with a DSSC to achieve zero bias water splitting with hydrogen evolution at a separate Pt dark cathode, figure 7 [153]. In a related approach, the added potential for proton/water reduction was provided by constructing a $\text{SnO}_2/\text{TiO}_2$ core-shell photoanode on the surface of a Si electrode [154]. Excitation of the assembly and electron transfer to the electrode were followed by electron transfer to Si and its activation to give H_2 at a separate Pt dark cathode. **Two electrode water splitting.** An extended version of figure 7, including a tandem DSPEC for H_2O splitting, is shown in figure 8. It combines a dye-sensitized photoanode and a dye-sensitized photocathode for light-driven water oxidation and reduction into O_2 and H_2 . In a recent report [144], an integrated double-electrode tandem cell for water splitting has been described. The cell consisted of a photoanode with a $\text{Ru}(\text{II})\text{bpy}/$

catalyst assembly on a core/shell $\text{SnO}_2/\text{TiO}_2$ electrode. The latter was integrated with the Si-based photocathode mentioned above. Under 1 sun illumination at pH 4.5, the cell was stable toward water splitting with a maximum photocurrent of $\sim 200\text{--}300 \mu\text{A cm}^{-2}$.

Advances in science and technology to meet challenges. Results to date have opened a door on a molecular assembly approach to solar water splitting. Continued progress in this area, ultimately with a goal of 10% solar efficiency for water splitting, has been significant. **Stability**—Progress has been made toward creating stable photoelectrode structures that persist for days, even for organic dyes. However, achieving catalytically stable structures, free of catalyst decomposition, remains a problem. An instability limit in current photoanodes for water oxidation arises from the use of derivatives of the Sun-based catalyst mentioned above because of slow surface dimerization. **Light absorption**—Covering as much of the solar spectrum as possible is a key in maximizing solar efficiency. Further research in this area is required to maximize the use of the solar distribution with

chromophore-catalyst combinations that maximize the efficiency of the solar input.

Concluding remarks. A review of progress made in this area is impressive. Using the band gap properties of semiconductors, and the excitation and catalytic properties

of molecular chromophores and catalysts has led to a systematic approach for the preparation of solar fuels. The molecular approach featured here has the advantage of using a chemical approach for the preparation of chromophores and catalysts with access to chemical synthesis for meeting the demands imposed by light absorption and catalysis.

8. Multiple exciton generation (MEG) from hot carriers for solar energy conversion

Arthur J Nozik^{1,2} and Matthew C Beard¹

¹National Renewable Energy Laboratory, United States of America

²University of Colorado, Boulder, CO, Department of Chemistry, 80309, United States of America

Status. Most current photovoltaic technologies are based upon conventional single junctions with power conversion efficiencies (PCEs) limited to 33%. New effects in nanostructured PV cells, such as efficient MEG have been demonstrated experimentally and have the potential to achieve PCEs well above 33%, as well as reduce module costs, but have not yet produced higher PCEs than conventional PV cells.

Current and future challenges. When photons with energies above the bandgap (E_g) of a semiconductor are absorbed they create electron–hole pairs that have excess kinetic energy above that of electrons and holes at the conduction and valence bandedges, respectively [155–188]. When these charge carriers equilibrate among themselves via electron–electron or hole–hole scattering to form Boltzmann distributions (a process termed thermalization), a carrier temperature can be assigned to them. These carriers are termed hot carriers; their maximum carrier temperature at the surface of the Earth is 3000 K under AM1.5 excitation at 1 sun intensity [156]. The hot carriers can cool to the lattice (ambient) temperature through carrier–phonon scattering, and thus convert their initial excess kinetic energy into heat through increased lattice vibrations. This hot carrier cooling process results in a loss of about 50% of the absorbed solar photon energy into heat and thus limits the maximum theoretical PCE of solar irradiance at 1 sun intensity into either electrical or chemical free energy (i.e. solar fuels) to 33% at 1 sun intensity [156, 183]; this maximum PCE value is named the S–Q limit after the authors who first derived it [183].

However, for maximizing the PCE for photovoltaic (PV) electricity, both the photovoltage and photocurrent are unconstrained and only their product is maximized, while for solar fuels the photovoltage is fixed and needs to be equal to the standard cell potential plus the overvoltage to drive the net reaction forward at a given rate. This latter constraint generally requires photovoltages above the optimum for PV PCE, and thus limits the S–Q PCE for solar fuels to below 33% at 1 sun intensity [184–186]. Notwithstanding, approaches to increase the PCE even above the S–Q limit are described below for both Solar Fuels and PV.

Hot carrier cooling rates in conventional semiconductors are very fast and their cooling to the lattice temperature which limits the PCE to 33% is generally completed in less than 1 ps [160, 161, 163, 165, 180, 181]; all free-energy converting solar cells in commercial use today generate electricity (photovoltaic (PV) cells) and operate with fully cooled hot

carriers that reside at their respective conduction and valence bandedges [186–188]. The direct conversion of solar irradiance into stored free energy in the chemical bonds of solar fuels by driving endoergic electrochemical oxidation–reduction reactions is readily demonstrated in the laboratory, but has not yet developed into a commercial solar fuels industry due to limitations on PCE, stability, and cost.

Advances in science and technology to meet challenges.

However, if hot carrier cooling in photoexcited semiconductors can be slowed down such that: (1) hot carriers are extracted before cooling and thus create higher photovoltages [155–159], or (2) the hot carriers can create additional electron–hole pairs through carrier multiplication [157, 164, 165, 184, 189–211] and thus create higher photocurrent, then their excess kinetic energy above the bandgap can be used to create additional electrical or chemical free energy and increase the PCE. Thus, the maximum S–Q thermodynamic PCE at one sun can be dramatically increased to > 65% for a hot-carrier solar cell with complete hot carrier extraction [156, 157, 165, 166], and >46% in the case of ideal carrier multiplication [184]. The difference occurs because for ideal carrier multiplication, conservation of energy requires that photons with energies between 1 and 2 times the bandgap can only generate heat and not multiple carriers, whereas for complete hot carrier extraction all carriers above $1E_g$ can be utilized to enhance free energy production. These approaches to high PV PCE have been labeled ‘Next (or Future) Generation Photovoltaics’ [165]. It is noted that a maximum PCE of 66% from complete hot carrier collection is the same as the limiting PCE of a large stack of conventional series-connected multijunction PV solar cells with descending bandgaps along the direction of the incident light, but the former is obtained with a single material rather than a complicated multiplicity of materials [184].

An effective and promising approach to slow the cooling of hot electrons is to utilize quantization effects in quantum-confined semiconductor nanostructures (i.e. QDs (3D confinement), quantum wires (2D confinement), and quantum films (1D confinement) [157, 164, 181, 184] (figures 9 and 10). In these nanostructures the creation of discrete electronic states with quantized energy level separations > phonon energies require simultaneous, and thus improbable, multi-phonon–electron scattering events to cool hot carriers. This approach is enhanced at high photon excitation densities wherein a high density of hot carriers can produce a high density of non-equilibrium (i.e. hot) phonons which cannot transmit their excitation energy to the lattice fast enough and instead feed energy back to the hot carrier population to keep it hot and slow the cooling [160–164, 208–210]. This effect is termed a ‘hot phonon bottleneck’. Another related approach is to use bulk semiconductors that have large differences in their acoustic and optical phonon energies (such as the III–nitrides), and thus block the transition of optical phonons into acoustic phonons which couple to the lattice in the last step of carrier cooling [167, 207].

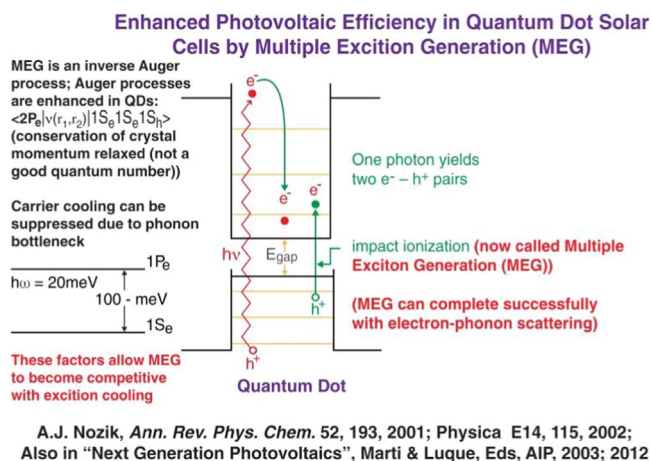


Figure 9. MEG in a quantum dot when $h\nu > 2E_g$.

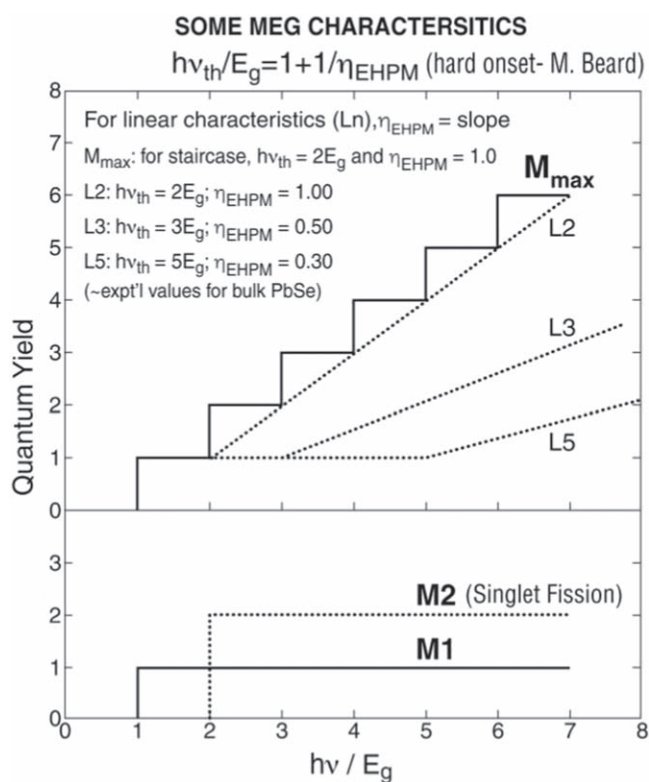


Figure 10. Ideal MEG characteristics where M_{max} produces N excitons/photon when $h\nu/E_g = N$. LN is a linear characteristic where the MEG energy threshold ($h\nu/E_g$) = N (2, 3, 4, etc) [197].

Slowed hot carrier cooling was first studied in 1D confined quantized structures, initially in the space charge layers of heavily doped semiconductors [155, 157–159] and then in quantum films (termed 1D quantum wells and superlattices) produced by gas phase epitaxy [157–164]; slowed cooling was only produced via a hot phonon bottleneck [157–164]. Over the past 20 years other quantized and non-quantized structures were studied in PV cells in attempts to realize the very high predicted PCE that would arise from hot carrier extraction [155–207]. Although hot

carrier effects were observed, the ultra-high PCEs have not yet been achieved.

An important advance in the R&D of Future Generation Solar Photon Conversion to electricity and solar fuels was the realization and experimental verification, beginning in the early 2000s, that in semiconductor nanostructures, initially in 3-dimensionally confined NCs (QDs) and later in all 3 types of spatial confinement in quantized NCs, carrier multiplication of absorbed photons could be nearly ideally efficient with a threshold of just twice the bandgap, the minimum photon energy required to satisfy energy conservation [164, 180, 184, 185, 189–206]. In NCs, the requirement to also satisfy momentum conservation in addition to energy conservation, is relaxed. This allows the threshold for carrier multiplication to occur at $2E_g$ [181], unlike the threshold for carrier multiplication in bulk semiconductors (termed impact ionization in the bulk case) where the threshold is $>3E_g$ to $>5E_g$ because of the need to also satisfy crystal momentum. Regarding PCE, in the most efficient NCs photons with energy $N \times E_g$ will produce N electron–hole pairs per photon, creating a staircase function of quantum yield with a unit increase of QY for every additional bandgap of absorbed photon energy. Finally, since photogenerated electron–hole pairs in NCs are created in a small nanoscale volume, the electron and hole interact strongly with each other and produce excitons that are stable at room temperature, rather than free carriers as in bulk semiconductors. Hence, multiplication of electron–hole pairs in NCs is referred to as MEG.

Recently, several important and interesting R&D developments have occurred, and are described below:

1. Theoretical analyses of solar PCE for both PV and solar fuels show that when MEG is combined with solar concentration the PCE soars to extremely high peak values but at substantially reduced bandgaps. For example, for single junction PV the peak PCE at 500 suns is 75% for $E_g = 0.2$ eV, and for $E_g = 0.6$ eV the peak PCE is 55% [202]. For solar fuels (e.g. H_2O splitting) in a two-bandgap photosystem cell in a Z-scheme with bandgaps of 0.8 and 1.2 eV, the PCE at an overvoltage of 0.4 V and with 500 suns is 48% [203]; at one sun it is about 35% [203].
2. New photomaterials called metal-halide perovskites (general formula ABX_3 , where A = cation 1, B = cation 2 (usually a metal), and X = a halide (or oxygen)) have been shown by many international researchers to exhibit remarkable opto-electronic properties, including high photovoltaic efficiencies close to Si solar cells [211–213] and exceptionally slow hot carrier cooling rates [208–210]. Regarding slow carrier cooling, various perovskites films of different composition are reported in over 70 recent papers to exhibit remarkably slow hot carrier cooling, both through a hot phonon bottle neck created with high photoexcitation intensity and without high intensity photoexcitation [208–210]. Some results show exceedingly slow hot carrier cooling time (>100 ps) [209, 210]. One attractive proposed reason for slow hot carrier cooling

is the rapid formation of polarons that screen the carriers from electron–phonon interactions, thus inhibiting this normally fast cooling mechanism [211–214]. Thus, there is widespread speculation that perovskite solar cells will be excellent candidates for hot carrier solar cells; MEG for solar fuels in non-perovskites cells has also been recently demonstrated [215].

possible to find systems that enable inexpensive and high efficient devices from QD-based inks. Surpassing the S–Q limit for a single-junction solar converter system is a scientific and technological challenge with significant benefits to society. The challenge is to increase the MEG efficiency to approach the energy conservation limit and produce PCEs close to the theoretical maxima.

Concluding remarks. QD solar cells remain a promising technology for inexpensive, scalable, and efficient solar cells. Such semiconductor nanostructures are synthesized in solution phase chemical reactions, where the reaction conditions can be modified to produce a variety of shapes, compositions, and structures. Thanks to their size- and surface-tunability and solution processing, it should be

Acknowledgments

Support from the Solar Photochemistry program within the Division of Chemical Sciences, Geosciences, and Biosciences in the Office of Basic Energy of the Department of Energy is acknowledged. DOE funding was provided to NREL through Contract DE-AC36-086038308.

9. Cascade biocatalysis in electrode nanopores

Clare F Megarity and Fraser A Armstrong

Department of Chemistry, University of Oxford, Oxford, United Kingdom

Status. Enzymes have long been established as efficient and specific catalysts, and it is now known that many behave as reversible electrocatalysts when attached to certain electrode materials, rivaling Pt for hydrogen evolution and even catalyzing CO₂ reduction with minimal overpotential [216]. Consequently, there have been extensive efforts to understand and mimic enzymes in the design of small catalysts for renewable energy conversions [217]. Because H₂ and carbon fuels have very low market values, their economic production from sunlight or renewable electricity demands catalysts that are inexpensive, robust and scalable, paradoxically ruling out isolated enzymes in any direct application. Enzymes have instead been used in demonstration devices (akin to ‘toys’) where their value has been to expose other steps of solar fuel production as rate-limiting factors, examples being where they are incorporated into colloidal semiconductor systems [218]. It is feasible, however, to implement enzymes directly for production and detection of high-value, specialty chemicals, and nanoscience has an important role to play—here, however, our interest is focused not on the internal properties of the solid nanostructures themselves but the confined spaces they generate when packed in three dimensions.

In living cells, enzyme reaction sequences (cascades) are localized in membrane-enclosed nanozones (lumens) having internal diameters <100 nm—familiar examples being the energy-processing organelles mitochondria and chloroplasts (figure 11(A)). One obvious advantage of nanoconfinement is that it produces a massive enhancement of rate, by concentrating the different enzymes (catalysts) and limiting distances across which intermediates and recycling mobile cofactors must diffuse: nanoconfinement is essential for life. How does technology exploit this trick? It is well known that nanoconfinement forms the basis for very selective catalysis in zeolites and metal organic frameworks, and nanoconfined enzymatic reactions also have been well reviewed [219]; but driving nanoconfined cascades *electrochemically* is a special, and particularly powerful case. Importantly, the solution is to exploit the tiny 3D interstitial spaces that are created when electronically conducting nanoparticles pack. A bio-nanomaterial hybrid technology, ‘the electrochemical leaf’, provides a new way to investigate and exploit biocatalysis, enabling enzyme-catalyzed reactions to be executed in an efficient and inexpensive manner, with continuous real-time monitoring and exquisite control [220, 221]. The fundamental science underpinning the discovery is that two (or more) different enzymes (E1, E2...) are confined within the network of nanopores (10–100 nm) in a conducting metal oxide (MO) layer that has been produced by electrophoretic deposition of nanoparticles on a suitable support, such as titanium foil, graphite, or indium tin oxide (ITO) glass. Commercially

available ITO nanoparticles are suitable for this purpose. The first of the enzymes, E1, is a photosynthetic flavoenzyme (FNR) which recycles the mobile nicotinamide cofactor (NADP(H)—biology’s hydride carrier, using electrons supplied to/from the electrode. The second enzyme (E2) may be one of hundreds of oxidoreductases (in the future to be produced by design, including directed evolution) that recycle the NADP(H) and selectively produce a desired product at a high rate. The resulting electrode is represented in the generic form (FNR + E2)@MO/support.

The role of FNR is central as it is a one-electron/two-electron (hydride) convertor: trapped in the pores, FNR represents the ‘engine’ that can be driven in forward or reverse directions by the electrode potential, to recycle nicotinamide cofactors that enter and may be concentrated in the pores, with inherent turnover frequencies exceeding 100 000 per hour. The overall current reports on rate-limiting downstream reactions through NADP(H) coupling to E2 that may extend to further steps through enzymes E3, E4 etc in a lengthy cascade (figure 11(B)). The combined action of two (or more) complementary enzymes bound in close proximity, in which one (E1 = FNR) functions as both energizer and reporter while the next in sequence (E2) recycles the product of FNR, distinguishes this technology from other nanoconfined catalysis. Only FNR is required to exchange electrons and thus have intimate tunneling contact with the electrode material—the other enzymes need only be confined close by. It is important also to recognize that the porous layer does not simply increase the surface area of the electrode, a key factor required to make fuel cells operate effectively.

So far, several small cascades have been demonstrated, each involving efficient and selective synthesis of a product by reduction or oxidation [221]. As well as driving the reactions with an instrumentally-generated electrode potential, oxidation or reduction can be driven and monitored through connection to a Pt electrode in contact with air or H₂ respectively [222].

Current and future challenges. A major gap in our understanding of the electrochemical leaf is the structure of the enzyme-loaded nanoporous ITO layer. So far, the technology has been ‘tried and tested’ but without atomic-level definition, and all current insight arises from extrapolation of a few facts. The size scale is clear from figure 11(C), which shows 2D cross-sectional ‘ant farm’ views of an ITO layer, adapted from scanning electron microscopy results. The FNR molecule alone is positively charged with a diameter of approximately 6 nm, and its electrostatic binding within an electrophoretically-deposited ITO layer (thickness 1–3 μm) is very favorable. Charge-by-integration examinations of the resulting reversible cyclic voltammetry of the active site flavin group reveal that a hypothetical and idealized (flat surface) coverage would exceed 10 monolayers at pH 8, rising to approximately 100 monolayers at pH 9. The peak-type voltammetric signals are nearly ideal for two rapid one-electron transfers with some radical stability [216], and the only interpretation is that FNR

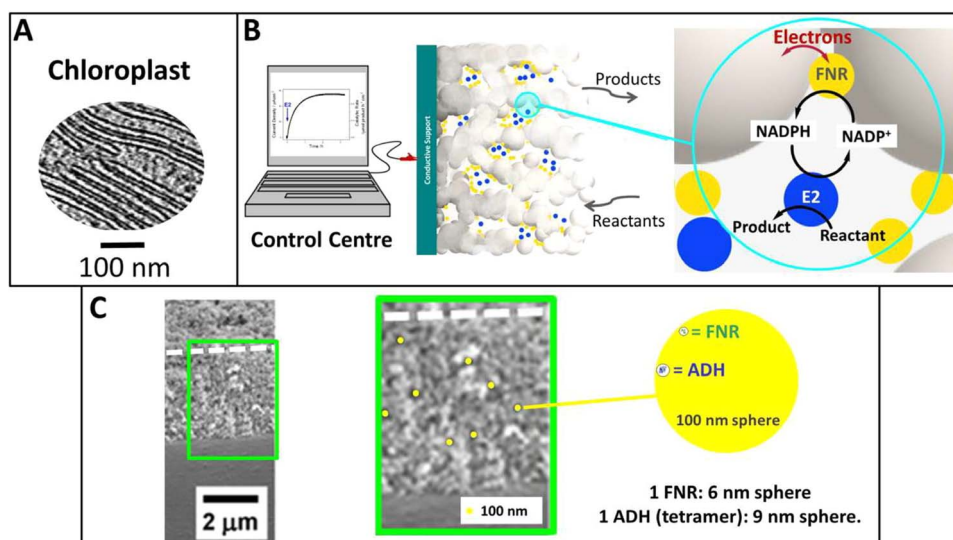


Figure 11. Extended electrocatalysis by nanoconfined enzyme cascades: (A), the inspiration; (B), the operational principle; (C), the internal nanopore landscape seen as an ‘ant farm’ based on 2D SEM cross sections and enzyme dimensions.

occupies many essentially equivalent sites deep into the layer, indeed a flat ITO glass electrode does not bind FNR [220]. This picture was quickly extended to include E2 as well [221]. Transmission electron microscopy revealed that the layer consists of ITO particles that are mainly in the diameter range 10–20 nm, but these have aggregated to form larger clusters that pack together densely to produce a random network of tunnels and chambers [221]. By necessity, the minimal functional catalytic unit has the composition [1 FNR + 1 nicotinamide + 1 E2], but the nanocavities can easily accommodate larger groups: indeed, the knowledge that altering FNR/E2 ratios leads to increased rates while cascades can be extended to include E3, E4., clearly demonstrates the flexible capacity of the nano-networks to host thriving enzyme communities. Such communities could change with time, either improving or decreasing the catalytic rate over hours and days—optimization thus being crucial. Enzyme size, shape, and charge will be important factors in determining their entry and mobility. Although the layer must be permeable to small reactants and products, the very fast conversion rates might challenge proton transfer or expose product inhibition that may not normally be seen. The normal concepts of the ionic double layer and electric field gradient are blurred in such a 3D electrode, where the entire modified material is the electrocatalyst.

Advances in science and technology to meet challenges.

Our understanding would benefit greatly from having a more uniform porous structure and quantification of each type of enzyme occupying reasonably defined nanozones. The first challenge might be met by using nanoparticles of a single fixed size and improving the layer formation, for example by advanced templating methods. Other types of conducting nanoparticles may produce better structural definition.

Regarding the second challenge, modern protein engineering methods ensure a large repertoire of cascades for developing the technology, and different enzymes of a cascade might be linked together, chemically or genetically, to obtain well-defined ratios and separation distances. Adoption of the technology will also be greatly extended by genetically engineering FNR to use the alternative nicotinamide cofactor NAD(H). Mathematical modeling, albeit based on ideal nanopore structures, will play an important role in understanding how the catalytic rates depend on so many variables.

Concluding remarks. The ‘electrochemical leaf’ is both concept and device: it offers opportunities outside nanoscience and electrochemistry—the basis being a vastly adaptable biohybrid material that is able to execute myriad organic transformations. The exquisite control that can be achieved over complex and often intractable biocatalytic cascades may prove to be important for biocatalyst discovery. The activity of any number of *non*-redox enzymes serving in a cascade can be detected easily even though they are not involved in electron transfer. The technology should be scalable, in which case it could also revolutionize the ‘green’ production of high-value organic molecules, including pharmaceuticals, that require NAD(P)(H) recycling.

Acknowledgments

C F M and F A A are supported by a grant (CF 327) from the EPA Cephalosporin Fund.

ORCID iDs

U Banin  <https://orcid.org/0000-0003-1698-2128>
 L Hammarström  <https://orcid.org/0000-0002-9933-9084>
 J Sá  <https://orcid.org/0000-0003-2124-9510>
 H Tian  <https://orcid.org/0000-0001-6897-2808>
 M B Johnston  <https://orcid.org/0000-0002-0301-8033>
 L M Herz  <https://orcid.org/0000-0001-9621-334X>
 M G Kanatzidis  <https://orcid.org/0000-0003-2037-4168>
 K L Kohlstedt  <https://orcid.org/0000-0001-8045-0930>
 G C Schatz  <https://orcid.org/0000-0001-5837-4740>
 N Lewis  <https://orcid.org/0000-0001-5245-0538>
 T Meyer  <https://orcid.org/0000-0002-7006-2608>
 A J Nozik  <https://orcid.org/0000-0001-7176-7645>
 M C Beard  <https://orcid.org/0000-0002-2711-1355>
 F Armstrong  <https://orcid.org/0000-0001-8041-2491>
 C A Schmittenmaer  <https://orcid.org/0000-0001-9992-8578>
 V S Batista  <https://orcid.org/0000-0002-3262-1237>
 G W Brudvig  <https://orcid.org/0000-0002-7040-1892>

References

- [1] Wu K and Lian T 2016 Quantum confined colloidal nanorod heterostructures for solar-to-fuel conversion *Chem. Soc. Rev.* **45** 3781–810
- [2] Ben-Shahar Y *et al* 2016 Optimal metal domain size for photocatalysis with hybrid semiconductor-metal nanorods *Nat. Commun.* **7** 10413
- [3] Stone D, Ben-Shahar Y, Waiskopf N and Banin U 2018 The metal type governs photocatalytic reactive oxygen species formation by semiconductor-metal hybrid nanoparticles *ChemCatChem* **10** 5119–23
- [4] Amirav L and Alivisatos A P 2010 Photocatalytic hydrogen production with tunable nanorod heterostructures *J. Phys. Chem. Lett.* **1** 1051–4
- [5] Ben-Shahar Y *et al* 2015 Effect of surface coating on the photocatalytic function of hybrid CdS–Au nanorods *Small* **11** 462–71
- [6] Perry D, Waiskopf N, Verbitsky L, Remennik S and Banin U 2019 Shell stabilization of photocatalytic ZnSe nanorods *ChemCatChem* **11** 6208–12
- [7] Yu S *et al* 2018 Efficient photocatalytic hydrogen evolution with ligand engineered all-inorganic InP and InP/ZnS colloidal quantum dots *Nat. Commun.* **9** 4009
- [8] Simon T *et al* 2014 Redox shuttle mechanism enhances photocatalytic H₂ generation on Ni-decorated CdS nanorods *Nat. Mater.* **13** 1013–8
- [9] Kalisman P, Nakibli Y and Amirav L 2016 Perfect photon-to-hydrogen conversion efficiency *Nano Lett.* **16** 1776–81
- [10] Han Z, Qiu F, Eisenberg R, Holland P L and Krauss T D 2012 Robust photogeneration of H₂ in water using semiconductor nanocrystals and a nickel catalyst *Science* **338** 1321–4
- [11] Ben-Shahar Y and Banin U 2016 Hybrid semiconductor-metal nanorods as photocatalysts *Top. Curr. Chem.* **374** 54
- [12] Wolff C M *et al* 2018 All-in-one visible-light-driven water splitting by combining nanoparticulate and molecular co-catalysts on CdS nanorods *Nat. Energy* **3** 862–9
- [13] Jia G, Pang Y, Ning J, Banin U and Ji B 2019 Heavy-metal-free colloidal semiconductor nanorods: recent advances and future perspectives *Adv. Mater.* **31** 1900781
- [14] Berr M J *et al* 2012 Hole scavenger redox potentials determine quantum efficiency and stability of Pt-decorated CdS nanorods for photocatalytic hydrogen generation *Appl. Phys. Lett.* **100** 223903
- [15] Panfil Y E, Oded M and Banin U 2018 Colloidal quantum nanostructures: emerging materials for display applications *Angew. Chem., Int. Ed.* **57** 4274–95
- [16] Ji B *et al* 2019 Strain-controlled shell morphology on quantum rods *Nat. Commun.* **10** 2
- [17] Ding T X, Olshansky J H, Leone S R and Alivisatos A P 2015 Efficiency of hole transfer from photoexcited quantum dots to covalently linked molecular species *J. Am. Chem. Soc.* **137** 2021–9
- [18] Weiss E A 2017 Designing the surfaces of semiconductor quantum dots for colloidal photocatalysis *ACS Energy Lett.* **2** 1005–13
- [19] Banin U and Ben-Shahar Y 2018 A hybrid solution *Nat. Energy* **3** 824–5
- [20] O'Regan B and Grätzel M 1991 A low-cost, high-efficiency solar-cell based in dye-sensitized colloidal TiO₂ films *Nature* **353** 737–40
- [21] Cao Y, Liu Y, Zakeeruddin S M, Hagfeldt A and Grätzel M 2018 Direct contact of selective charge extraction layers enables high-efficiency molecular photovoltaics *Joule* **2** 1108–17
- [22] Hao Y, Yang W, Zhang L, Jiang R, Mijangos E, Saygili Y, Hammarström L, Hagfeldt A and Boschloo G 2016 A small electron donor in cobalt complex electrolyte significantly improves efficiency in dye-sensitized solar cells *Nat. Commun.* **7** 13934
- [23] Wang P, Yang L, Wu H, Cao Y, Zhang J, Xu N, Chen S, Decoppet J-D, Zakeeruddin S M and Grätzel M 2018 Stable and efficient organic dye-sensitized solar cell based on ionic liquid electrolyte *Joule* **2** 2145–53
- [24] Robel L, Kuno M and Kamat P V 2007 Size-dependent electron injection from excited CdSe quantum dots into TiO₂ nanoparticles *J. Am. Chem. Soc.* **128** 4136–7
- [25] Kojima A, Teshima K, Shirai Y and Miyasaka T 2009 Organometal halide perovskites as visible-light sensitizers for photovoltaic cells *J. Am. Chem. Soc.* **131** 6050–1
- [26] Zhang X, Liu J, Zhang J, Vlachopoulos N and Johansson E M J 2015 ZnO@Ag₂S core-shell nanowire arrays for environmentally friendly solid-state quantum dot-sensitized solar cells with panchromatic light capture and enhanced electron collection *Phys. Chem. Chem. Phys.* **17** 12786–95
- [27] Sá J, Tagliabue G, Friedli P, Szlachetko J, Rittmann-Frank M H, San-Tomauro F G, Milne C J and Sigg H 2013 Direct observation of charge separation on Au localized surface plasmons *Energy Environ. Sci.* **6** 3584–8
- [28] Hattori Y, Abdallah M, Meng J, Zheng K and Sá J 2019 Simultaneous hot electron and hole injection upon excitation of gold surface plasmon *J. Phys. Chem. Lett.* **10** 3140–6
- [29] Nakamura K, Oshikiri T, Ueno K, Wang Y, Kamata Y, Kotake Y and Misawa H 2016 Properties of plasmon-induced photoelectric conversion on a TiO₂/NiO p–n junction with Au nanoparticles *J. Phys. Chem. Lett.* **7** 1004–9
- [30] Nikolaou V, Charisiadis A, Charalambidis G, Coutsolelos A and Odobel F 2017 Recent advances and insights in dye-sensitized NiO photocathodes for photovoltaic devices *J. Mater. Chem.* **5** 21077–113
- [31] Gibson E A, Smeigh A L, Le Pleux L, Boschloo G, Blart E, Pellegrin Y, Odobel F, Hagfeldt A and Hammarström L 2009 A p-type NiO-based dye-sensitized solar cell with a Voc of 0.35 V *Angew. Chem.* **48** 4402–5
- [32] Tian H 2019 Solid-state p-type dye-sensitized solar cells: progress, potential applications and challenges *Sustain. Energy Fuels* **3** 888–98
- [33] Burschka J, Dualah A, Kessler F, Baranoff E, Cevy-Ha N-L, Yi C, Nazeeruddin M K and Grätzel M 2011 Tris(2-(1H-pyrazol-1-yl)pyridine)cobalt(III) as p-type dopant for

- organic semiconductors and its application in highly efficient solid-state dye-sensitized solar cells *J. Am. Chem. Soc.* **133** 18042–5
- [34] Freitag M, Daniel Q, Pazoki M, Sveinbjörnsson K, Zhang J, Sun L, Hagfeldt A and Boschloo G 2015 High-efficiency dye-sensitized solar cells with molecular copper phenanthroline as solid hole conductor *Energy Environ. Sci.* **8** 2634–7
- [35] Zhang W *et al* 2018 Comprehensive control of voltage loss enables 11.7% efficient solid-state dye-sensitized solar cells *Energy Environ. Sci.* **11** 1779–87
- [36] Dhillon S S *et al* 2017 *J. Phys. D: Appl. Phys.* **50** 043001
- [37] Beard M C, Turner G M and Schmittenmaer C A 2002 *Nano Lett.* **2** 983–7
- [38] Jepsen P U, Schairer W, Libon I H, Lemmer U, Hecker N E, Birkholz M, Lips K and Schall M 2001 *Appl. Phys. Lett.* **79** 1291–3
- [39] Joyce H J, Boland J L, Davies C L, Baig S A and Johnston M B 2016 *Semicond. Sci. Technol.* **31** 103003
- [40] Milot R L, Eperon G E, Green T, Snaith H J, Johnston M B and Herz L M 2016 *J. Phys. Chem. Lett.* **7** 4178–84
- [41] Wehrenfennig C, Eperon G E, Johnston M B, Snaith H J and Herz L M 2014 *Adv. Mater.* **26** 1584–9
- [42] Buizza L R V, Crothers T W, Wang Z, Patel J B, Milot R L, Snaith H J, Johnston M B and Herz L M 2019 *Adv. Funct. Mater.* **29** 1902656
- [43] Motti S G, Crothers T, Yang R, Cao Y, Li R, Johnston M B, Wang J and Herz L M 2019 *Nano Lett.* **19** 3953–60
- [44] Joyce H J *et al* 2012 *Nano Lett.* **12** 5325–30
- [45] Turner G M, Beard M C and Schmittenmaer C A 2002 *J. Phys. Chem. B* **106** 11716–9
- [46] Milot R L and Schmittenmaer C A 2015 *Acc. Chem. Res.* **48** 1423–31
- [47] Tiwana P, Docampo P, Johnston M B, Snaith H J and Herz L M 2011 *ACS Nano* **5** 5158–66
- [48] Lee S H, Regan K P, Hedstrom S, Matula A J, Chaudhuri S, Crabtree R H, Batista V S, Schmittenmaer C A and Brudvig G W 2017 *J. Phys. Chem. C* **121** 22690–9
- [49] Tiwana P, Docampo P, Johnston M B, Herz L M and Snaith H J 2012 *Energy Environ. Sci.* **5** 9566–73
- [50] Moore G F, Blakemore J D, Milot R L, Hull J F, Song H E, Cai L, Schmittenmaer C A, Crabtree R H and Brudvig G W 2011 *Energy Environ. Sci.* **4** 2389–92
- [51] Lloyd-Hughes J and Jeon T I 2012 *J. Infrared Millim. Terahertz Waves* **33** 871–925
- [52] Mooshammer F *et al* 2018 *Nano Lett.* **18** 7515–23
- [53] Cocker T L, Jelic V, Gupta M, Molesky S J, Burgess J A J, De Los Reyes G, Titova L V, Tsui Y Y, Freeman M R and Hegmann F A 2013 *Nat. Photon.* **7** 620–5
- [54] Nemes C T, Koenigsmann C and Schmittenmaer C A 2015 *J. Phys. Chem. Lett.* **6** 3257–62
- [55] Seifert T *et al* 2016 *Nat. Photon.* **10** 483–8
- [56] Manser J S, Christians J A and Kamat P V 2016 Intriguing optoelectronic properties of metal halide perovskites *Chem. Rev.* **116** 12956
- [57] Chung I, Lee B, He J, Chang R P and Kanatzidis M G 2012 All-solid-state dye-sensitized solar cells with high efficiency *Nature* **485** 486
- [58] Stoumpos C C and Kanatzidis M G 2015 The renaissance of halide perovskites and their evolution as emerging semiconductors *Acc. Chem. Res.* **48** 2791
- [59] Kim H S *et al* 2012 Lead iodide perovskite sensitized all-solid-state submicron thin film mesoscopic solar cell with efficiency exceeding 9% *Sci. Rep.* **2** 591
- [60] Lee M M, Teuscher J, Miyasaka T, Murakami T N and Snaith H J 2012 Efficient hybrid solar cells based on meso-structured organometal halide perovskites *Science* **338** 643
- [61] National Renewable Energy Laboratory. Research Cell Record Efficiency Chart, 2020 (<https://nrel.gov/pv/assets/pdfs/best-research-cell-efficiencies.20200803.pdf>) (accessed: 13 August, 2020)
- [62] Lal N N, Dkhissi Y, Li W, Hou Q, Cheng Y-B and Bach U 2017 Perovskite tandem solar cells *Adv. Energy Mater.* **7** 1602761
- [63] Leijtens T *et al* 2018 Tin–lead halide perovskites with improved thermal and air stability for efficient all-perovskite tandem solar cells *Sustain. Energy Fuels* **2** 2450
- [64] Hao F, Stoumpos C C, Chang R P H and Kanatzidis M G 2014 Anomalous band gap behavior in mixed Sn and Pb perovskites enables broadening of absorption spectrum in solar cells *J. Am. Chem. Soc.* **136** 8094
- [65] Bush K A *et al* 2017 23.6%-efficient monolithic perovskite/silicon tandem solar cells with improved stability *Nat. Energy* **2** 17009
- [66] Shen H *et al* 2018 Mechanically-stacked perovskite/CIGS tandem solar cells with efficiency of 23.9% and reduced oxygen sensitivity *Energy Environ. Sci.* **11** 394
- [67] Correa-Baena J-P, Abate A, Saliba M, Tress W, Jesper Jacobsson T, Grätzel M and Hagfeldt A 2017 The rapid evolution of highly efficient perovskite solar cells *Energy Environ. Sci.* **10** 710
- [68] Eperon G E, Hörantner M T and Snaith H J 2017 Metal halide perovskite tandem and multiple-junction photovoltaics *Nat. Rev. Chem.* **1** 0095
- [69] Chen Y, Sun Y, Peng J, Zhang W, Su X, Zheng K, Pullerits T and Liang Z 2017 Tailoring organic cation of 2D air-stable organometal halide perovskites for highly efficient planar solar cells *Adv. Energy Mater.* **7** 1700162
- [70] Li T, Pan Y, Wang Z, Xia Y, Chen Y and Huang W 2017 Additive engineering for highly efficient organic–inorganic halide perovskite solar cells: recent advances and perspectives *J. Mater. Chem. A* **5** 12602
- [71] Misra R K, Aharon S, Layani M, Magdassi S and Etgar L 2016 A mesoporous–planar hybrid architecture of methylammonium lead iodide perovskite based solar cells *J. Mater. Chem. A* **4** 14423
- [72] Tan H *et al* 2017 Efficient and stable solution-processed planar perovskite solar cells via contact passivation *Science* **355** 722
- [73] Dunlap-Shohl W A, Zhou Y, Pature N P and Mitzi D B 2019 Synthetic approaches for halide perovskite thin films *Chem. Rev.* **119** 3193
- [74] Körbel S, Marques M A L and Botti S 2018 Stable hybrid organic–inorganic halide perovskites for photovoltaics from ab initio high-throughput calculations *J. Mater. Chem. A* **6** 6463
- [75] Tsai H *et al* 2016 High-efficiency two-dimensional Ruddlesden–Popper perovskite solar cells *Nature* **536** 312
- [76] Yang R *et al* 2018 Oriented quasi-2D perovskites for high performance optoelectronic devices *Adv. Mater.* **30** 1804771
- [77] Liu Y *et al* 2019 Ultrahydrophobic 3D/2D fluoroarene bilayer-based water-resistant perovskite solar cells with efficiencies exceeding 22% *Sci. Adv.* **5** eaaw2543
- [78] Snaith H J 2018 Present status and future prospects of perovskite photovoltaics *Nat. Mater.* **17** 372
- [79] Zhao D *et al* 2017 Low-bandgap mixed tin–lead iodide perovskite absorbers with long carrier lifetimes for all-perovskite tandem solar cells *Nat. Energy* **2** 17018
- [80] Stoumpos C C, Malliakas C D and Kanatzidis M G 2013 Semiconducting tin and lead iodide perovskites with organic cations: phase transitions, high mobilities, and near-infrared photoluminescent properties *Inorg. Chem.* **52** 9019
- [81] Ma Z-Q, Pan H, Wong P K and First-Principles A 2016 Study on the structural and electronic properties of Sn-based organic–inorganic halide perovskites *J. Electron. Mater.* **45** 5956
- [82] Huang L-Y and Lambrecht W R L 2013 Electronic band structure, phonons, and exciton binding energies of halide

- perovskites CsSnCl₃, CsSnBr₃, and CsSnI₃ *Phys. Rev. B* **88** 165203
- [83] Wang F, Ma J, Xie F, Li L, Chen J, Fan J and Zhao N 2016 Organic cation-dependent degradation mechanism of organotin halide perovskites *Adv. Funct. Mater.* **26** 3417
- [84] Dong Q, Liu F, Wong M K, Tam H W, Djurišić A B, Ng A, Surya C, Chan W K and Ng A M C 2016 Encapsulation of perovskite solar cells for high humidity conditions *ChemSusChem* **9** 2597
- [85] Cheacharoen R, Boyd C C, Burkhard G F, Leijtens T, Raiford J A, Bush K A, Bent S F and McGehee M D 2018 Encapsulating perovskite solar cells to withstand damp heat and thermal cycling *Sustain. Energy Fuels* **2** 2398
- [86] Reese M O *et al* 2011 Consensus stability testing protocols for organic photovoltaic materials and devices *Sol. Energy Mater. Sol. Cells* **95** 1253
- [87] Zhu J *et al* 2014 Towards Service Lifetime Prediction of Photovoltaic Modules, Towards Service Lifetime Prediction of Photovoltaic Modules (https://nrel.gov/pv/assets/pdfs/2014_pvmrw_59_zhu.pdf)
- [88] Passarelli J V, Fairfield D J, Sather N A, Hendricks M P, Sai H, Stern C L and Stupp S I 2018 Enhanced out-of-plane conductivity and photovoltaic performance in *n* = 1 layered perovskites through organic cation design *J. Am. Chem. Soc.* **140** 7313
- [89] Spanopoulos I, Ke W, Stoumpos C C, Schueller E C, Kontsevoi O Y, Seshadri R and Kanatzidis M G 2018 Unraveling the chemical nature of the 3D ‘Hollow’ hybrid halide perovskites *J. Am. Chem. Soc.* **140** 5728
- [90] Spanopoulos I *et al* 2019 Uniaxial expansion of the 2D Ruddlesden–Popper perovskite family for improved environmental stability *J. Am. Chem. Soc.* **141** 5518
- [91] Guilbert A A Y *et al* 2017 Quantitative analysis of the molecular dynamics of P3HT:PCBM bulk heterojunction *J. Phys. Chem. B* **121** 9073–80
- [92] Movaghar B, Jones L O, Ratner M A, Schatz G C and Kohlstedt K L 2019 Are transport models able to predict charge carrier mobilities in organic semiconductors? *J. Phys. Chem. C* **123**
- [93] Jackson N E *et al* 2015 Conformational order in aggregates of conjugated polymers *J. Am. Chem. Soc.* **137** 6254–62
- [94] Padula D, Simpson J D and Troisi A 2019 Combining electronic and structural features in machine learning models to predict organic solar cells properties *Mater. Horiz.* **6** 343–9
- [95] Alessandri R *et al* 2017 Bulk heterojunction morphologies with atomistic resolution from coarse-grain solvent evaporation simulations *J. Am. Chem. Soc.* **139** 3697–705
- [96] Greco C *et al* 2019 Generic model for lamellar self-assembly in conjugated polymers: linking mesoscopic morphology and charge transport in P3HT *Macromolecules* **52** 968–81
- [97] Jackson N E, Chen L X and Ratner M A 2016 Charge transport network dynamics in molecular aggregates *Proc. Natl Acad. Sci.* **113** 8595–600
- [98] Swick S M, Gebraad T, Jones L, Fu B, Aldrich T J, Kohlstedt K L, Schatz G C, Facchetti A and Marks T J 2019 Building blocks for high-efficiency organic photovoltaics: interplay of molecular, crystal, and electronic properties in post-fullerene ITIC ensembles *ChemPhysChem* **20** 2608–26
- [99] Cui Y *et al* 2019 Over 16% efficiency organic photovoltaic cells enabled by a chlorinated acceptor with increased open-circuit voltages *Nat. Commun.* **10** 2515
- [100] <https://nrel.gov/pv/cell-efficiency.html>
- [101] Peng Z *et al* 2018 Measuring temperature-dependent miscibility for polymer solar cell blends: an easily accessible optical method reveals complex behavior *Chem. Mater.* **30** 3943–51
- [102] Gagorik A G *et al* 2017 Improved scaling of molecular network calculations: the emergence of molecular domains *J. Phys. Chem. Lett.* **8** 415–21
- [103] Savoie B M *et al* 2014 Mesoscale molecular network formation in amorphous organic materials *Proc. Natl Acad. Sci.* **111** 10055–60
- [104] Wang S W *et al* 2019 Polymerization-enhanced two-photon photosensitization for precise photodynamic therapy *ACS Nano* **13** 3095–105
- [105] Lewis N S 2017 Developing a scalable artificial photosynthesis technology through nanomaterials by design *Nat. Nanotechnol.* **11** 1010–9
- [106] McKone J R, Lewis N S and Gray H B 2014 Will solar-driven water-splitting devices see the light of day? *Chem. Mater.* **26** 407–14
- [107] Ager J W, Shaner M R, Walczak K A, Sharp I D and Ardo S 2015 Experimental demonstrations of spontaneous, solar-driven photoelectrochemical water splitting *Energy Environ. Sci.* **8** 2811–24
- [108] Verlage E, Hu S, Liu R, Jones R J R, Sun K, Xiang C X, Lewis N S and Atwater H A 2015 A monolithically integrated, intrinsically safe, 10% efficient, solar-driven water-splitting system based on active, stable earth-abundant electrocatalysts in conjunction with tandem III–V light absorbers protected by amorphous TiO₂ films *Energy Environ. Sci.* **8** 3166–72
- [109] Cheng W H, Richter M H, May M M, Ohlmann J, Lackner D, Dimroth F, Hannappel T, Atwater H A and Lewerenz H J 2018 Monolithic photoelectrochemical device for direct water splitting with 19% efficiency *ACS Energy Lett.* **3** 1795–800
- [110] McCrory C C L, Jung S, Ferrer I M, Chatman S M, Peters J C and Jaramillo T F 2015 Benchmarking hydrogen evolving reaction and oxygen evolving reaction electrocatalysts for solar water splitting devices *J. Am. Chem. Soc.* **137** 4347–57
- [111] Moreno-Hernandez I A, MacFarland C A, Read C G, Papadantonakis K M, Brunshwig B S and Lewis N S 2017 Crystalline nickel manganese antimonate as a stable water-oxidation catalyst in aqueous 1.0 M H₂SO₄ *Energy Environ. Sci.* **10** 2103–8
- [112] Benck J D, Hellstern T R, Kibsgaard J, Chakthranont P and Jaramillo T F 2014 Catalyzing the hydrogen evolution reaction (HER) with molybdenum sulfide nanomaterials *ACS Catal.* **4** 3957–71
- [113] Kibsgaard J and Jaramillo T F 2014 Molybdenum Phosphosulfide: an active, acid-stable, earth-abundant catalyst for the hydrogen evolution reaction *Angew. Chem., Int. Ed.* **53** 14433–7
- [114] Xiang C X, Papadantonakis K M and Lewis N S 2016 Principles and implementations of electrolysis systems for water splitting *Mater. Horiz.* **3** 169–73
- [115] Chen Y K, Hu S, Xiang C X and Lewis N S 2015 A sensitivity analysis to assess the relative importance of improvements in electrocatalysts, light absorbers, and system geometry on the efficiency of solar-fuels generators *Energy Environ. Sci.* **8** 876–86
- [116] Sun K, Ritzert N L, John J, Tan H Y, Hale W G, Jiang J J, Moreno-Hernandez I, Papadantonakis K M, Moffat T P and Brunshwig B S 2018 Performance and failure modes of Si anodes patterned with thin-film Ni catalyst islands for water oxidation *Sustain. Energy Fuels* **2** 983–98
- [117] Brinkert K, Richter M H, Akay O, Liedtke J, Giersig M, Fountaine K T and Lewerenz H J 2018 Efficient solar hydrogen generation in microgravity environment *Nat. Commun.* **9** 2527
- [118] Singh M R, Papadantonakis K M, Xiang C X and Lewis N S 2015 An electrochemical engineering assessment of the operational conditions and constraints for solar-driven water-splitting systems at near-neutral pH *Energy Environ. Sci.* **8** 2760–7

- [119] Bard A J and Wrighton M S 1977 Thermodynamic potential for the anodic dissolution of n-type semiconductors *J. Electrochem. Soc.* **124** 1706–10
- [120] Hu S, Lewis N S, Ager J W, Yang J H, McKone J R and Strandwitz N C 2014 Thin-film materials for the protection of semiconducting photoelectrodes in solar-fuel generators *J. Phys. Chem. C* **119** 24201–28
- [121] Fujishima A and Honda K 1972 Electrochemical photolysis of water at a semiconductor electrode *Nature* **238** 37–8
- [122] Bock C R, Connor J A, Gutierrez A R, Meyer T J, Whitten D G, Sullivan B P and Nagle J K 1979 Estimation of excited-state redox potentials by electron-transfer quenching. Application of electron-transfer theory to excited-state redox processes *J. Am. Chem. Soc.* **101** 4815–24
- [123] Concepcion J J, Jurss J W, Templeton J L and Meyer T J 2008 Mediator-assisted water oxidation by the ruthenium 'blue dimer' cis,cis-[(bpy)₂(H₂O)RuORu(OH₂)(bpy)₂]⁴⁺ *Proc. Natl Acad. Sci. USA* **105** 17632–5
- [124] Binstead R A, Moyer B A, Samuels G J and Meyer T J 1981 Proton-coupled electron transfer between [Ru(bpy)₂(py)OH₂]²⁺ and [Ru(bpy)₂(py)O]²⁺. A solvent isotope effect (kH₂O/kD₂O) of 16.1 *J. Am. Chem. Soc.* **103** 2897–9
- [125] Meshitsuka S, Ichikawa M and Tamaru K 1974 Electro catalysis by metal phthalocyanines in the reduction of carbon dioxide *J. Chem. Soc., Chem. Commun.* 158–9
- [126] Fisher B J and Eisenberg R 1980 Electro catalytic reduction of carbon dioxide by using macrocycles of nickel and cobalt *J. Am. Chem. Soc.* **102** 7361–3
- [127] Hawecker J, Lehn J-M and Ziessel R 1984 Electro catalytic reduction of carbon dioxide mediated by Re(bipy)(CO)₃Cl (bipy=2,2'-bipyridine) *J. Chem. Soc., Chem. Commun.* 328–30
- [128] Sullivan B P, Bolinger C M, Conrad D, Vining W J and Meyer T J 1985 One- and two-electron pathways in the electro catalytic reduction of CO₂ by fac-Re(bpy)(CO)₃Cl (bpy=2,2'-bipyridine) *J. Chem. Soc., Chem. Commun.* 1414–6
- [129] Curtis J C, Bernstein J S and Meyer T J 1985 Directed, intramolecular electron transfer in mixed-valence dimers *Inorg. Chem.* **24** 385–97
- [130] Schanze K S, Neyhart G A and Meyer T J 1986 Excited-state electron transfer in ligand-bridged dimeric complexes of osmium *J. Phys. Chem.* **90** 2182–93
- [131] Denisevich P, Abruna H D, Leidner C R, Meyer T J and Murray R W 1982 Electropolymerization of vinylpyridine and vinylbipyridine complexes of iron and ruthenium: homopolymers, copolymers, reactive polymers *Inorg. Chem.* **21** 2153–61
- [132] O'Regan B and Gratzel M 1991 A low-cost, high-efficiency solar cell based on dye-sensitized colloidal TiO₂ films *Nature* **353** 737–40
- [133] Treadway J A, Moss J A and Meyer T J 1999 Visible region photooxidation on TiO₂ with a chromophore-catalyst molecular assembly *Inorg. Chem.* **38** 4386–7
- [134] Youngblood W J, Lee S-H A, Kobayashi Y, Hernandez-Pagan E A, Hoertz P G, Moore T A, Moore A L, Gust D and Mallouk T E 2009 Photoassisted overall water splitting in a visible light-absorbing dye-sensitized photoelectrochemical cell *J. Am. Chem. Soc.* **131** 926–7
- [135] Brennaman M K, Dillon R J, Alibabaei L, Gish M K, Dares C J, Ashford D L, House R L, Meyer G J, Papanikolas J M and Meyer T J 2016 Finding the way to solar fuels with dye-sensitized photoelectrosynthesis cells *J. Am. Chem. Soc.* **138** 13085–102
- [136] Zigler D F *et al* 2016 Disentangling the physical processes responsible for the kinetic complexity in interfacial electron transfer of excited Ru(II) polypyridyl dyes on TiO₂ *J. Am. Chem. Soc.* **138** 4426–38
- [137] Alibabaei L, Sherman B D, Norris M R, Brennaman M K and Meyer T J 2015 Visible photoelectrochemical water splitting into H₂ and O₂ in a dye-sensitized photoelectrosynthesis cell *Proc. Natl Acad. Sci. USA* **112** 5899–902
- [138] Ashford D L, Gish M K, Vannucci A K, Brennaman M K, Templeton J L, Papanikolas J M and Meyer T J 2015 Molecular chromophore-catalyst assemblies for solar fuel applications *Chem. Rev.* **115** 13006–49
- [139] Lapides A M, Sherman B D, Brennaman M K, Dares C J, Skinner K R, Templeton J L and Meyer T J 2015 Synthesis, characterization, and water oxidation by a molecular chromophore-catalyst assembly prepared by atomic layer deposition. The 'mummy' strategy *Chem. Sci.* **6** 6398–406
- [140] Shan B, Sherman B D, Klug C M, Nayak A, Marquard S L, Liu Q, Bullock R M and Meyer T J 2017 Modulating hole transport in multilayered photocathodes with derivatized p-type nickel oxide and molecular assemblies for solar-driven water splitting *J. Phys. Chem. Lett.* **8** 4374–9
- [141] Zhang L, Favereau L, Farre Y, Maufroy A, Pellegrin Y, Blart E, Hissler M, Jacquemin D, Odobel F and HamMarstrom L 2016 Molecular-structure control of electron transfer dynamics of push-pull porphyrins as sensitizers for NiO based dye sensitized solar cells *RSC Adv.* **6** 77184–94
- [142] Shan B, Farnum B H, Wee K and Meyer T J 2017 Generation of long-lived redox equivalents in self-assembled bilayer structures on metal oxide electrodes *J. Phys. Chem. C* **121** 5882–90
- [143] Shan B, Das A K, Marquard S, Farnum B H, Wang D, Bullock R M and Meyer T J 2016 Photogeneration of hydrogen from water by a robust dye-sensitized photocathode *Energy Environ. Sci.* **9** 3693–7
- [144] Shan B, Brennaman M K, Troian-Gautier L, Liu Y, Nayak A, Klug C M, Li T-T, Bullock R M and Meyer T J 2019 A silicon-based heterojunction integrated with a molecular excited state in a water-splitting tandem cell *J. Am. Chem. Soc.* **141** 10390–8
- [145] Shan B, Vanka S, Li T-T, Troian-Gautier L, Brennaman M K, Mi Z and Meyer T J 2019 Binary molecular- semiconductor p-n junctions for photoelectro catalytic CO₂ reduction *Nat. Energy* **4** 290–9
- [146] Hanson K, Losego M D, Kalanyan B, Ashford D L, Parsons G N and Meyer T J 2013 Stabilization of [Ru(bpy)₂(4,4'-(PO₃H₂)bpy)]²⁺ on mesoporous TiO₂ with atomic layer deposition of Al₂O₃ *Chem. Mater.* **25** 3–5
- [147] Xiao D, Martini L A, Snoeberger R C, Crabtree R H and Batista V S 2011 Inverse design and synthesis of acacoumarin anchors for robust TiO₂ sensitization *J. Am. Chem. Soc.* **133** 9014–22
- [148] Young K J, Martini L A, Milot R L, Snoeberger R C, Batista V S, Schmuttenmaer C A, Crabtree R H and Brudvig G W 2012 Light-driven water oxidation for solar fuels *Coord. Chem. Rev.* **256** 2503–20
- [149] Eberhart M S, Wang D, Sampaio R N, Marquard S L, Shan B, Brennaman M K, Meyer G J, Dares C and Meyer T J 2017 Water photo-oxidation initiated by surface-bound organic chromophores *J. Am. Chem. Soc.* **139** 16248–55
- [150] Duan L, Bozoglian F, Mandal S, Stewart B, Privalov T, Lobet A and Sun L 2012 A molecular ruthenium catalyst with water-oxidation activity comparable to that of photosystem II *Nat. Chem.* **4** 418–23
- [151] Wang D, Marquard S L, Troian-Gautier L, Sheridan M V, Sherman B D, Wang Y, Eberhart M S, Farnum B H, Dares C J and Meyer T J 2018 Interfacial deposition of Ru(II) bipyridine-dicarboxylate complexes by ligand substitution for applications in water oxidation catalysis *J. Am. Chem. Soc.* **140** 719–26
- [152] Sahara G, Kumagai H, Maeda K, Kaeffer N, Artero V, Higashi M, Abe R and Ishitani O 2016 Photoelectrochemical

- reduction of CO₂ coupled to water oxidation using a photocathode with a Ru(II)–Re(I) complex photocatalyst and a CoO_x/TaON photoanode *J. Am. Chem. Soc.* **138** 14152–8
- [153] Sherman B D, Sheridan M V, Wee K-R, Marquard S L, Wang D, Alibabaei L, Ashford D L and Meyer T J 2016 A dye-sensitized photoelectrochemical tandem cell for light driven hydrogen production from water *J. Am. Chem. Soc.* **138** 16745–53
- [154] Sheridan M V, Hill D J, Sherman B D, Wang D, Marquard S L, Wee K-R, Cahoon J F and Meyer T J 2017 All-in-one derivatized tandem p+n-silicon–SnO₂/TiO₂ water splitting photoelectrochemical cell *Nano Lett* **17** 2440–6
- [155] Boudreaux D S, Williams F and Nozik A J 1980 Hot carrier injection at semiconductor-electrolyte junctions *J. Appl. Phys.* **51** 2158–63
- [156] Ross R T and Nozik A J 1982 Efficiency of hot-carrier solar energy converters *J. Appl. Phys.* **53** 3813–8
- [157] Nozik A J 2001 Spectroscopy and hot electron relaxation dynamics in semiconductor quantum wells and quantum dots *Ann. Rev. Phys. Chem.* **52** 193–231
- [158] Turner J A and Nozik A J 1982 Evidence for hot-electron injection across p-GaP/electrolyte junctions *Appl. Phys. Lett.* **41** 101–3
- [159] Cooper G, Turner J A, Parkinson B A and Nozik A J 1983 Hot carrier injection of photogenerated electrons at indium phosphide-electrolyte interfaces *J. Appl. Phys.* **54** 6463–73
- [160] Pelouch W S, Ellingson R J, Powers P E, Tang C L, Szymd D M and Nozik A J 1992 Comparison of hot-carrier relaxation in quantum wells and bulk GaAs at high carrier densities *Phys. Rev. B* **45** 1450–3
- [161] Rosenwaks Y, Hanna M C, Levi D H, Szymd D M, Ahrenkiel R K and Nozik A J 1993 Hot carrier cooling in GaAs: quantum wells versus bulk *Phys. Rev. B* **48** 14675–8
- [162] Hanna M C, Zhengao L and Nozik A J 1997 Hot carrier solar cells *AIP Conf. Proc.* **404** 309
- [163] Edelstein D C, Tang C L and Nozik A J 1987 Picosecond relaxation of hot-carrier distributions in GaAs/GaAsP strained-layer superlattices *Appl. Phys. Lett.* **51** 48–50
- [164] Nozik A J 2002 Quantum dot solar cells *Physica E* **14** 115–20
- [165] Green M A 2006 *Third Generation Photovoltaics* (Berlin/Heidelberg: Springer)
- [166] Würfel P 1997 Solar energy conversion with hot electrons from impact ionization *Sol. Energy Mater. Sol. Cells* **46** 43–52
- [167] Conibeer G *et al* 2010 Modelling of hot carrier solar cell absorbers *Sol. Energy Mater. Sol. Cells* **94** 1516–21
- [168] Le Bris A *et al* 2012 Thermalisation rate study of GaSb-based heterostructures by continuous wave photoluminescence and their potential as hot carrier solar cell absorbers *Energy Environ. Sci.* **5** 6225–32
- [169] Hirst L C, Walters R J, Führer M F and Ekins-Daukes N J 2014 Experimental demonstration of hot-carrier photocurrent in an InGaAs quantum well solar cell *Appl. Phys. Lett.* **104** 231115
- [170] Rodière J, Lombez L, Le Corre A, Durand O and Guillemoles J-F 2015 Experimental evidence of hot carriers solar cell operation in multi-quantum wells heterostructures *Appl. Phys. Lett.* **106** 183901
- [171] Esmailpour H *et al* 2016 Suppression of phonon-mediated hot carrier relaxation in type-II InAs/AlAs_xSb_{1-x} quantum wells: a practical route to hot carrier solar cells *Prog. Photovolt., Res. Appl.* **24** 591–9
- [172] Zhang Y *et al* 2016 Extended hot carrier lifetimes observed in bulk In_{0.265±0.02}Ga_{0.735}N under high-density photoexcitation *Appl. Phys. Lett.* **108** 131904
- [173] Gibelli F, Lombez L and Guillemoles J-F 2017 Accurate radiation temperature and chemical potential from quantitative photoluminescence analysis of hot carrier populations *J. Phys.: Condens. Matter* **29** 06LT02
- [174] Esmailpour H *et al* 2017 Effect of occupation of the excited states and phonon broadening on the determination of the hot carrier temperature from continuous wave photoluminescence in InGaAsP quantum well absorbers *Prog. Photovolt., Res. Appl.* **25** 782–90
- [175] Dimmock J A R, Day S, Kauer M, Smith K and Heffernan J 2014 Demonstration of a hot-carrier photovoltaic cell *Prog. Photovolt., Res. Appl.* **22** 151–60
- [176] Dimmock J A R *et al* 2016 Optoelectronic characterization of carrier extraction in a hot carrier photovoltaic cell structure *J. Opt.* **18** 074003
- [177] Dimmock J A R, Kauer M, Smith K, Liu H, Stavrinou P N and Ekins-Daukes N J 2016 Optoelectronic characterization of carrier extraction in a hot carrier photovoltaic cell structure *J. Opt.* **18** 74003
- [178] Kirk A P and Fischetti M V 2012 Fundamental limitations of hot-carrier solar cells *Phys. Rev. B* **86** 165206
- [179] Ferry D K 2019 In search of a true hot carrier solar cell *Semicond. Sci. Technol.* **34** 044001
- [180] Nozik A J, Conibeer G and Beard M C (ed) 2014 *Advanced Concepts in Photovoltaics* (Cambridge: RSC)
- [181] Beard M C, Ip A H, Luther J M, Sargent E H and Nozik A J 2014 Quantum confined semiconductors for enhancing solar photoconversion through multiple exciton generation *Advanced Concepts in Photovoltaics* ed A J Nozik *et al* (Cambridge: RSC) ch 12, pp 345–78
- [182] Nguyen T, Lombez L, Gibelli F, Boyer-Richard S, Le Corre A, Durand O and Guillemoles J-F 2018 Quantitative experimental assessment of hot carrier enhanced solar cells at room temperature *Nature Energy* **3** 236–42
- [183] Shockley W and Queisser H J 1961 Detailed balance limit of efficiency of p–n junction solar cells *J. Appl. Phys.* **32** 510–9
- [184] Hanna M C and Nozik A J 2006 Solar conversion efficiency of photovoltaic and photoelectrolysis cells with carrier multiplication absorbers *J. Appl. Phys.* **100** 074510
- [185] Nozik A J 2013 Novel approaches to water splitting by solar photons *Photoelectrochemical Water Splitting: Issues and Perspectives* ed H J Lewerenz and L M Peter (Cambridge: Royal Soc Chem) ch 15
- [186] DeVos A 2008 *Thermodynamics of Solar Energy Conversion* (New York: Wiley) p 205
- [187] Würfel P 2002 Thermodynamic limitations to solar energy conversion *Physica E* **14** 18–26
- [188] Nozik A J 1978 Photoelectrochemistry: applications to solar energy conversion *Annu. Rev. Phys. Chem.* **29** 189–222
- [189] Schaller R and Klimov V L 2004 High efficiency carrier multiplication in PbSe nanocrystals: implications for solar energy conversion *Phys. Rev. Lett.* **92** 186601
- [190] Ellingson R J, Beard M C, Johnson J, Yu P, Mičić O I, Nozik A J, Shaehev A J and Efros A L 2005 Highly efficient multiple exciton generation in colloidal PbSe and PbS quantum dots *Nano Lett.* **5** 865–71
- [191] Nozik A J 2005 Exciton multiplication and relaxation dynamics in quantum dots: applications to ultrahigh-efficiency solar photon conversion *Inorg. Chem.* **44** 6893–9
- [192] Murphy J E, Beard M C, Norman A G, Ahrenkiel S P, Johnson J C, Yu P, Mičić O I, Ellingson R J and Nozik A J 2006 PbTe colloidal nanocrystals: synthesis, characterization, and multiple exciton generation *J. Am. Chem. Soc.* **128** 3241–7
- [193] Shabaev A L, Efros and Nozik A J 2006 Multi-exciton generation by a single photon in nanocrystals *Nano Lett.* **6** 2856–63
- [194] Nozik A J 2008 Multiple exciton generation in semiconductor quantum dots *Chem. Phys. Lett., Front. Chem.* **457** 3–11
- [195] Beard M C, Knutsen K K, Yu P, Luther J, Song Q, Ellingson R J and Nozik A J 2007 Multiple exciton generation in colloidal silicon nanocrystals *Nano Lett.* **7** 2506–12

- [196] Nozik A J 2010 Perspective article 'Nanoscience and nanostructures for photovoltaics and solar fuels' *Nano Lett.* **10** 2735–41
- [197] Beard M C, Midgett A G, Hanna M C, Luther J M, Hughes B K and Nozik A J 2010 Comparing multiple exciton generation in quantum dots to impact ionization in bulk semiconductors: implications for enhancement of solar energy conversion *Nano Lett.* **10** 3019–27
- [198] Nozik A J, Beard M C, Luther J M, Law M, Ellingson R J and Johnson J C 2010 Semiconductor quantum dots and quantum dot arrays and applications of MEG to 3rd generation PV solar cells *Chem. Rev. Thematic Issue* **110** 6873
- [199] Semonin O E, Luther J M, Choi S, Chem H-Y, Gao J, Nozik A J and Beard M 2011 Peak external photocurrent quantum efficiency exceeding 100% via MEG in a quantum dot solar cell', *Science* **334** 1530
- [200] Stewart J T, Padilha L, Qazilbash L A, Mumtaz M, Pietryga J M, Midgett A G, Luther L M, Beard M C, Nozik A J and Klimov V I 2012 Comparison of carrier multiplication yields in PbS and PbSe nanocrystals: the role of competing energy loss processes *Nano Lett.* **12** 622
- [201] Nozik A J 2012 Separating multiple excitons *Nat. Photon.* **6** 271
- [202] Hanna M C, Beard M and Nozik A J 2012 Effect of solar concentration on the thermodynamic power conversion efficiency of quantum dot solar cells exhibiting multiple exciton generation *J. Phys. Chem. Lett.* **3** 2857
- [203] Martinez M, Nozik A J and Beard M C 2019 Theoretical limits of MEG and singlet fission tandem devices for solar H₂O splitting *J. Chem. Phys.* **151** 114111
- [204] Beard M C, Luther J M, Semonin O and Nozik A J 2013 Third generation photovoltaics based on multiple exciton generation in quantum confined semiconductors *Acc. Chem. Res.* **46** 1252
- [205] Beard M C, Luther J M and Nozik A J 2014 The promise and challenge of nanostructured solar cells *Nat. Nanotechnol.* **9** 951
- [206] Kroupa D M *et al* 2018 Enhanced multiple exciton generation in PbS/CdS janus-like heterostructured nanocrystals *ACS Nano* **12** 10084–94
- [207] Conibeer G, Guillemoles J-F, Yu F and Levard H 2014 Hot carrier solar cells *Advanced Concepts in Photovoltaics* ed A J Nozik *et al* (Cambridge: RSC) ch 12, pp 379–421
- [208] Yang Y, Ostrowski D P, France R M, Zhu K, van de Lagemaat J, Matthew C and Beard M C 2016 Observation of a hot-phonon bottleneck in lead-iodide perovskites *Nat. Photon.* **10** 53–9
- [209] Kahmann S and Loi M A 2019 Hot carrier solar cells and the potential of perovskites for breaking the Shockley–Queisser limit *J. Mater. Chem. C* **7** 2471
- [210] Li M, Fu J, Xu Q and Sum T 2018 Slow hot-carrier cooling in halide perovskites: prospects for hot carrier solar cells *Adv. Mater.* **31** 1802486
- [211] Saliba M, Correa-Baena J-P, Graetzel M, Hagfeldt A and Abate A 2018 Perovskite solar cells: from the atomic level to film quality and device performance *Angew. Chem., Int. Ed.* **57** 2554–69
- [212] Park N-G 2014 Perovskite solar cells *Advanced Concepts in Photovoltaics* ed A J Nozik *et al* (Cambridge: RSC) pp 242–57
- [213] Zhu H and Zhu X Y 2016 Screening in crystalline liquids protects energetic carriers in hybrid perovskites *Science* **353** 1409
- [214] Evans T J S and Zhu X Y 2018 Competition between hot-electron cooling and large polaron screening in CsPbBr₃ perovskites *J. Phys. Chem. C* **122** 13724–30
- [215] Yan Y, Crisp R, Gu J, Chernomordik B D, Pach G F, Marshall A R, Turner J A and Beard M C 2017 Multiple exciton generation for photoelectrochemical hydrogen evolution with quantum yields exceeding 100% *Nat. Energy* **2** 17052
- [216] Evans R M, Siritanaratkul B, Megarity C F, Pandey K, Esterle T F, Badiani S and Armstrong F A 2019 *Chem. Soc. Rev.* **48** 2039
- [217] Artero V 2017 *Nat. Energy* **2** 17131
- [218] Kornienko N, Zhang J Z, Sakimoto K K, Yang P and Reisner E 2018 *Nat. Nanotechnol.* **13** 890
- [219] K uchler A, Yoshimoto M, Luginb uhl S, Mavelli F and Walde P 2016 *Nat. Nanotechnol.* **11** 409
- [220] Siritanaratkul B, Megarity C F, Roberts T G, Samuels T O M, Winkler M, Warner J H, Happe T and Armstrong F A 2017 *Chem. Sci.* **8** 4579
- [221] Megarity C F *et al* 2019 *Angew. Chem., Int. Ed.* **58** 4948
- [222] Wan L, Megarity C F, Siritanaratkul B and Armstrong F A 2018 *Chem. Commun.* **54** 972